

RESEARCH

Open Access



High-accuracy quasi-variable mesh method for the system of 1D quasi-linear parabolic partial differential equations based on off-step spline in compression approximations

RK Mohanty^{1*} and Sachin Sharma²

*Correspondence:

rmohanty@sau.ac.in

¹Department of Applied Mathematics, South Asian University, Akbar Bhawan, Chanakyapuri, New Delhi 110021, India

Full list of author information is available at the end of the article

Abstract

In this article, we propose a new two-level implicit method of accuracy two in time and three in space based on spline in compression approximations using two off-step points and a central point on a quasi-variable mesh for the numerical solution of the system of 1D quasi-linear parabolic partial differential equations. The new method is derived directly from the continuity condition of the first-order derivative of the spline function. The stability analysis for a model problem is discussed. The method is directly applicable to problems in polar systems. To demonstrate the strength and utility of the proposed method, we solve the generalized Burgers-Fisher equation, generalized Burgers-Huxley equation, coupled Burgers-equations and heat equation in polar coordinates. We demonstrate that the proposed method enables us to obtain high accurate solution for high Reynolds number.

MSC: 65M06; 65M12; 65M22; 65Y20

Keywords: quasi-linear parabolic equations; quasi-variable mesh; spline in compression; generalized Burgers-Fisher equations; coupled Burgers equation; Newton's iterative method

1 Introduction

We consider the one-space dimensional quasi-linear parabolic partial differential equation (PDE) of the form

$$u_{xx} = f(x, t, u, u_x, u_t), \quad 0 < x < 1, t > 0. \quad (1.1)$$

The initial and boundary conditions are given by

$$u(x, 0) = u_0(x), \quad 0 \leq x \leq 1, \quad (1.2)$$

$$u(0, t) = g_0(t), \quad u(1, t) = g_1(t), \quad t > 0, \quad (1.3)$$

where we assume that the functions $f, u_0(x), g_0(t)$ and $g_1(t)$ are sufficiently smooth and their required higher-order derivatives exist.

The quasi-linear parabolic equation describes a wide class of physical phenomenon such as the interaction between reaction mechanism, convection, effects and diffusion transports. It is used in many fields such as chemistry, biology, metallurgy and engineering. The one-dimensional viscous generalized Burgers-Fisher equation (GBFE) and generalized Burgers-Huxley equation (GBHE) are famous examples of quasi-linear parabolic equations.

The GBFE is given by

$$\varepsilon u_{xx} = u_t + \alpha u^\delta u_x + \beta u(u^\delta - 1), \quad t > 0, \tag{1.4}$$

where α, β are real parameters, δ is a positive integer and $0 < \varepsilon \leq 1$.

The GBHE is given by

$$\varepsilon u_{xx} = u_t + \alpha u^\delta u_x + \beta u(u^\delta - 1)(u^\delta - \gamma), \quad t > 0, \tag{1.5}$$

where $\alpha, \beta \geq 0, \gamma \in (0, 1), \delta > 0$ and $0 < \varepsilon \leq 1$ are the parameters.

In both cases, equations describe the interaction between diffusion, convection and reaction.

The GBFE has wide applications in the fields such as gas dynamics, fluid mechanics, elasticity, heat conduction and plasma physics. The well-known equation (1.4) was first used by Fisher [1] to describe the propagation of gene in a habitat. In his memory, it is generally referred as Fisher’s equation. When $\alpha = 0$ and $\delta = 1$, equation (1.4) reduces to the classical Fisher equation. Kolmogorov *et al.* [2] independently wrote down the same equation to describe the dynamic spread of a combustion front. This equation has been found in various contexts in which a perturbation spreads in an excitable medium.

The GBHE was investigated by Satsuma *et al.* [3] in 1987. When $\varepsilon = 1, \alpha = 0, \delta = 1$, equation (1.5) reduces to the Huxley equation and describes nerve pulse propagation in nerve fibers and wall motion in liquid crystals. For $\varepsilon = 1, \beta = 0$, equation (1.5) reduces to the generalized Burgers equation, which describes the far field of wave propagation in nonlinear dissipative systems. When $\varepsilon = 1, \alpha = 0, \beta = 1$ and $\delta = 1$, equation (1.5) becomes the Fitz-Hugh-Nagumo (FHN) equation which is the reaction diffusion equation used in circuit theory and biology. When $\alpha \neq 0, \beta \neq 0$ and $\delta = 1$, equation (1.5) turns into the Burgers-Huxley equation (BHE) and shows a prototype model for describing the interaction between diffusion transports, convection and reaction mechanisms.

There has been vast variety of numerical methods, such as finite element methods, finite difference methods, spectral techniques and finite volume methods for quasi-linear parabolic initial-boundary value problems. In recent years, various numerical methods were used by the researchers to solve GBHE and GBFE. A fourth-order scheme for GBHE was proposed by Bratsos [4]. Mohammadi [5] has discussed a spline method for GBFE. Zhang *et al.* [6] solved GBFE using the local discontinuous Galerkin method. Diaz [7] analysed the solitary wave solution of the BHE through Cardano’s method. Mittal and Tripathi [8] discussed the schemes using collocation of cubic B-splines for numerical solutions of GBFE and GBHE. A two-level implicit compact operator method of order two in time and four in space was discussed for the approximate solution of time dependent BHE by Mohanty *et al.* [9].

Higher-order finite difference methods on a uniform mesh for the solution of nonlinear parabolic equations were proposed by Jain *et al.* [10]. Mittal and Jiwari [11] developed differential quadrature method for numerical solution of coupled viscous Burgers' equations. Mohanty *et al.* [12] used compact operator technique to solve coupled Burgers' equations. In recent past, Talwar *et al.* [13] proposed spline in compression method based on three full-step grid points for the solution of 1D quasi-linear parabolic equations and in those methods the consistency equation is only second-order accurate and the method is not directly applicable to singular problems, which is a main drawback of those methods. To the best of the authors' knowledge, no numerical method of order two in time and three in space, directly obtained from the consistency condition, for the solution of parabolic equation (1.1) on a quasi-variable mesh has been discussed in the literature so far.

In this paper, using a central point and two off-step points in x -direction, we propose a new two-level implicit method of accuracy two in time and three in space, based on spline in compression approximations for the solution of differential equation (1.1). The proposed method is obtained directly from the consistency condition and is of order three in space. Difficulties were experienced in the past for the higher-order spline solution of parabolic equation in polar coordinates. The solution usually deteriorates in the vicinity of the singularity. A special technique is required to handle such problems, whereas the proposed method is directly applicable to solve singular problems without any modification, which is the main attraction of our work. Our paper is arranged as follows: In Section 2, we discuss the non-polynomial spline in compression function and its properties on a quasi-variable mesh. In Section 3, we give derivation of the method. In Section 4, we generalize the proposed method for the system of quasi-linear parabolic PDEs. Stability analysis for model problem is discussed and it is shown that the linear scheme is unconditionally stable in Section 5. In this section, we also discuss the stability analysis for a fourth-order parabolic equation which is consistent with system of 1D quasi-linear parabolic PDEs. In Section 6, numerical results are presented for some benchmark problems with tabular and graphical illustrations and compare the results with the results obtained by other researchers. Final remarks are given in Section 7.

2 Spline in compression approximations and its properties

For the approximate solution of the initial-boundary value problems (1.1)-(1.3), we discretize the space interval $[0, 1]$ as $0 = x_0 < x_1 < \dots < x_N < x_{N+1} = 1$, where N is a positive integer. The spline approximation consists of two off-step points $x_{l\pm 1/2}$ and a central point x_l , $l = 0, 1, 2, \dots, N$ with two end points x_0 and x_{N+1} , where $h_l = x_l - x_{l-1}$, $l = 1, 2, \dots, N + 1$, be the mesh size in x -direction and $k = t_{j+1} - t_j > 0$, $j = 0, 1, 2, \dots$ be the mesh spacing in t -direction. Spatial grid points are defined by $x_l = x_0 + \sum_{i=1}^l h_i$, $l = 1(1)N + 1$, and the time steps are given by $t_j = jk$, $j = 0(1)J$, where J is a positive integer. The mesh ratio is denoted by $\sigma_l = (h_{l+1}/h_l) > 0$, $l = 1(1)N$. The neighboring off-step points are defined as $x_{l-1/2} = x_l - \frac{h_l}{2}$ and $x_{l+1/2} = x_l + \frac{\sigma_l h_l}{2}$, $l = 1(1)N$. For $\sigma_l = 1$, it reduces to the uniform mesh case. Let $U_l^j = u(x_l, t_j)$ be the exact solution value of $u(x, t)$ and is approximated by u_l^j . For simplicity, we consider $\sigma_l = \sigma$ (a constant $\neq 1$), $l = 1(1)N$. For $\sigma > 1$ or $\sigma < 1$, the mesh sizes are either increasing or decreasing in order. Such a mesh is called a quasi-variable mesh.

A non-polynomial spline function of degree 3 which interpolate u_l^j at j th level is given by

$$P_j(x) = a_l^j + b_l^j(x - x_l) + c_l^j \sin w(x - x_l) + d_l^j \cos w(x - x_l), \quad x_{l-1} \leq x \leq x_l, \quad (2.1)$$

which satisfy the following conditions at j th time level:

- (i) $P_j(x) \in C^2[0, 1]$, and
- (ii) $P_j(x_l) = U_l^j, P_j(x_{l-1}) = U_{l-1}^j$, where w is an arbitrary parameter and $P_j'(x_l) = M_l^j = U_{xxl}^j, P_j''(x_{l\pm 1}) = M_{l\pm 1}^j = U_{xxl\pm 1}^j, P_j''(x_{l\pm 1/2}) = M_{l\pm 1/2}^j = U_{xxl\pm 1/2}^j, l = 0(1)N + 1, j > 0$.

The derivatives of non-polynomial spline function $P_j(x)$ for $x \in [x_{l-1}, x_l]$ are given by

$$P_j'(x) = b_l^j + wc_l^j \cos w(x - x_l) - wd_l^j \sin w(x - x_l), \tag{2.2}$$

$$P_j''(x) = -w^2[c_l^j \sin w(x - x_l) + d_l^j \cos w(x - x_l)]. \tag{2.3}$$

Using the conditions described above with algebraic calculations, we obtain the coefficients

$$a_l^j = U_l^j + \frac{M_l^j}{w^2}, \quad b_l^j = \frac{U_l^j - U_{l-1}^j}{h_l} + \frac{M_l^j}{w\mu_l} - \frac{M_{l-1/2}^j}{w\mu_l} \cos \mu_l,$$

$$c_l^j = \frac{M_{l-1/2}^j - M_l^j \cos \mu_l}{w^2 \sin \mu_l}, \quad d_l^j = -\frac{M_l^j}{w^2}.$$

Here $\mu_l = \frac{wh_l}{2}$.

Substituting the coefficients $a_l^j, b_l^j, c_l^j, d_l^j$, in equation (2.1), we obtain the non-polynomial spline in compression function

$$P_j(x) = U_l^j + \frac{M_l^j}{w^2} + \left(\frac{U_l^j - U_{l-1}^j}{h_l} + \frac{M_l^j}{w\mu_l} - \frac{M_{l-1/2}^j}{w\mu_l} \cos \mu_l \right) (x - x_l)$$

$$+ \left(\frac{M_{l-1/2}^j - M_l^j \cos \mu_l}{w^2 \sin \mu_l} \right) \sin w(x - x_l) - \frac{M_l^j}{w^2} \cos w(x - x_l), \quad x \in [x_{l-1}, x_l]. \tag{2.4}$$

Similarly, we get

$$P_j(x) = U_l^j + \frac{M_l^j}{w^2} + \left(\frac{U_{l+1}^j - U_l^j}{h_{l+1}} - \frac{M_l^j}{w\mu_{l+1}} + \frac{M_{l+1/2}^j}{w\mu_{l+1}} \cos \mu_{l+1} \right) (x - x_l)$$

$$+ \left(\frac{M_l^j \cos \mu_{l+1} - M_{l+1/2}^j}{w^2 \sin \mu_{l+1}} \right) \sin w(x - x_l)$$

$$- \frac{M_l^j}{w^2} \cos w(x - x_l), \quad x \in [x_l, x_{l+1}]. \tag{2.5}$$

On differentiating equations (2.4) and (2.5), we get

$$P_j'(x) = \frac{U_l^j - U_{l-1}^j}{h_l} + \frac{M_l^j}{w\mu_l} - \frac{M_{l-1/2}^j}{w\mu_l} \cos \mu_l$$

$$+ \left(\frac{M_{l-1/2}^j - M_l^j \cos \mu_l}{w \sin \mu_l} \right) \cos w(x - x_l)$$

$$+ \frac{M_l^j}{w^2} \sin w(x - x_l), \quad x \in [x_{l-1}, x_l] \tag{2.6}$$

and

$$\begin{aligned}
 P'_j(x) &= \frac{U_{l+1}^j - U_l^j}{h_{l+1}} - \frac{M_l^j}{w\mu_{l+1}} + \frac{M_{l+1/2}^j}{w\mu_{l+1}} \cos \mu_{l+1} \\
 &\quad + \left(\frac{M_l^j \cos \mu_{l+1} - M_{l+1/2}^j}{w \sin \mu_{l+1}} \right) \cos w(x - x_l) \\
 &\quad + \frac{M_l^j}{w^2} \sin w(x - x_l), \quad x \in [x_l, x_{l+1}].
 \end{aligned}
 \tag{2.7}$$

Using the continuity of the first derivative, that is, $P'_j(x_{l-}) = P'_j(x_{l+})$, we obtain the consistency condition

$$\frac{U_{l+1}^j - (1 + \sigma)U_l^j + \sigma U_{l-1}^j}{\sigma h_l^2} = [\alpha_l M_{l+1/2}^j + (\beta_{1l} + \beta_{2l})M_l^j + \gamma_l M_{l-1/2}^j] + T_l^j, \quad l = 1(1)N, \tag{2.8}$$

where

$$\alpha_l = \frac{\sigma}{2\mu_{l+1}^2} \left[\frac{\mu_{l+1}}{\sin \mu_{l+1}} - \cos \mu_{l+1} \right] = \frac{\sigma}{3} - \frac{\sigma^3 \mu_l^2}{90} + O(\mu_l^4), \tag{2.9a}$$

$$\beta_{1l} = \frac{\sigma}{2\mu_{l+1}^2} (1 - \mu_{l+1} \cot \mu_{l+1}) = \frac{\sigma}{6} + \frac{\sigma^3 \mu_l^2}{90} + O(\mu_l^4), \tag{2.9b}$$

$$\beta_{2l} = \frac{1}{2\mu_l^2} (1 - \mu_l \cot \mu_l) = \frac{1}{6} + \frac{\mu_l^2}{90} + O(\mu_l^4), \tag{2.9c}$$

$$\gamma_l = \frac{1}{2\mu_l^2} \left[\frac{\mu_l}{\sin \mu_l} - \cos \mu_l \right] = \frac{1}{3} - \frac{\mu_l^2}{90} + O(\mu_l^4), \tag{2.9d}$$

and $T_l^j = O(h_l^3)$.

On equating the coefficients of M_l^j in (2.8), we obtain the condition

$$\alpha_l + \beta_{1l} + \beta_{2l} + \gamma_l = \frac{(1 + \sigma)}{2} + O(\mu_l^4). \tag{2.10}$$

Using (2.9a)-(2.9d) in equation (2.8), we get the consistency condition in the following form:

$$\begin{aligned}
 &U_{l+1}^j - (1 + \sigma)U_l^j + \sigma U_{l-1}^j \\
 &= \sigma h_l^2 \left[\left(\frac{\sigma}{3} - \frac{\sigma^3 \mu_l^2}{90} \right) M_{l+1/2}^j + \frac{(1 + \sigma)}{6} M_l^j + \frac{(1 + \sigma^3) \mu_l^2}{90} M_l^j + \left(\frac{1}{3} - \frac{\mu_l^2}{90} \right) M_{l-1/2}^j \right] \\
 &\quad + O(h_l^5) \\
 &= \frac{\sigma h_l^2}{3} \left[\sigma M_{l+1/2}^j + \frac{(1 + \sigma)}{2} M_l^j + M_{l-1/2}^j \right] \\
 &\quad - \frac{\sigma h_l^2 \mu_l^2}{90} \left[\sigma^3 M_{l+1/2}^j + M_{l-1/2}^j - (1 + \sigma^3) M_l^j \right] + O(h_l^5).
 \end{aligned}
 \tag{2.11}$$

Since the term $\frac{\sigma h_l^2 \mu_l^2}{90} [\sigma^3 M_{l+1/2}^j + M_{l-1/2}^j - (1 + \sigma^3) M_l^j]$ is of $O(h_l^5)$, simplifying (2.11), we obtain the consistency condition

$$U_{l+1}^j - (1 + \sigma)U_l^j + \sigma U_{l-1}^j = \frac{\sigma h_l^2}{3} \left[\sigma M_{l+1/2}^j + \frac{(1 + \sigma)}{2} M_l^j + M_{l-1/2}^j \right] + O(h_l^5). \tag{2.12}$$

Further, substituting the values of (2.9a)-(2.9d) in (2.10) and neglecting $O(\mu_l^4)$ terms, we get

$$\tan(\mu_l/2) = \mu_l/2. \tag{2.13}$$

The above equation has an infinite number of roots, the smallest positive non-zero root being given by $\mu_l = \mu = 8.986818916$. When $w \rightarrow 0$, then $(\alpha_l, \beta_{1l}, \beta_{2l}, \gamma_l) \rightarrow (\frac{\sigma}{3}, \frac{\sigma}{6}, \frac{1}{6}, \frac{1}{3})$, and equation (2.8) reduces to a cubic spline relation.

Further, from equations (2.6)-(2.7), we get

$$P_j'(x_{l-1/2}) = \frac{U_l^j - U_{l-1}^j}{h_l} + \frac{(M_l^j - M_{l-1/2}^j \cos \mu_l)}{w \mu_l} + \frac{(M_{l-1/2}^j - M_l^j \cos \mu_l)}{w \sin \mu_l} \cos \mu_l - \frac{M_l^j}{w} \sin \mu_l, \tag{2.14}$$

and

$$P_j'(x_{l+1/2}) = \frac{U_{l+1}^j - U_l^j}{\sigma h_l} - \frac{(M_l^j - M_{l+1/2}^j \cos \mu_{l+1})}{w \mu_{l+1}} + \frac{(M_l^j \cos \mu_{l+1} - M_{l+1/2}^j)}{w \sin \mu_{l+1}} \cos \mu_{l+1} + \frac{M_l^j}{w} \sin \mu_{l+1}. \tag{2.15}$$

Simplifying (2.14) and (2.15), we obtain

$$P_j'(x_{l-1/2}) = \frac{U_l^j - U_{l-1}^j}{h_l} - \frac{h_l}{4} (2\beta_{2l} M_l^j - \gamma_l M_{l-1/2}^j), \tag{2.16}$$

$$P_j'(x_{l+1/2}) = \frac{U_{l+1}^j - U_l^j}{\sigma h_l} + \frac{h_l}{4} (2\beta_{1l} M_l^j - \alpha_l M_{l+1/2}^j). \tag{2.17}$$

Equations (2.16) and (2.17) are two important properties of non-polynomial spline in compression function $P_j(x)$.

3 Derivation of the numerical method

For the derivation of the method, we simply follow the approaches given by Mohanty [14].

At the grid point (x_l, t_j) , let us denote

$$U_{pq} = \frac{\partial^{p+q} U}{\partial x^p \partial t^q}, \quad \alpha_l^j = \frac{\partial f}{\partial u}, \quad \beta_l^j = \frac{\partial f}{\partial u_x}, \quad \gamma_l^j = \frac{\partial f}{\partial u_t}, \quad \delta_l^j = \frac{\partial f}{\partial t}. \tag{3.1}$$

Differentiating the differential equation (1.1) partially with respect to 't' at the grid point (x_l, t_j) , we obtain a relation

$$-\gamma_l^j U_{02} = \delta_l^j + U_{01} \alpha_l^j + U_{11} \beta_l^j - U_{21}. \tag{3.2}$$

At the grid point (x_l, t_j) , we can write the differential equation as

$$M_l^j = f(x_l, t_j, U_l^j, U_{xl}^j, U_{ul}^j). \tag{3.3}$$

Similarly,

$$M_{l+1/2}^j = f(x_{l+1/2}, t_j, U_{l+1/2}^j, U_{xl+1/2}^j, U_{ul+1/2}^j), \tag{3.4}$$

$$M_{l-1/2}^j = f(x_{l-1/2}, t_j, U_{l-1/2}^j, U_{xl-1/2}^j, U_{ul-1/2}^j). \tag{3.5}$$

Since M_l^j and $M_{l\pm 1/2}^j$ contain the first derivative terms, from the consistency condition (2.12), the non-polynomial spline in compression method for the parabolic equation (1.1) can be written as

$$[\bar{U}_{l+1}^j - (1 + \sigma)\bar{U}_l^j + \sigma\bar{U}_{l-1}^j] = \frac{\sigma h_l^2}{3} \left[\sigma \hat{M}_{l+1/2}^j + \frac{(1 + \sigma)}{2} \hat{M}_l^j + \hat{M}_{l-1/2}^j \right] + \hat{T}_l^j, \tag{3.6}$$

where $\hat{T}_l^j \equiv O(kh_l^3 + h_l^5)$, provided $\sigma \neq 1$ and we use the following approximations:

$$\bar{t}_j = t_j + \theta k, \tag{3.7}$$

$$\bar{U}_l^j = \theta U_l^{j+1} + (1 - \theta)U_l^j = U_l^j + \theta k U_{01} + O(k^2), \tag{3.8}$$

$$\bar{U}_{l+1}^j = \theta U_{l+1}^{j+1} + (1 - \theta)U_{l+1}^j = U_{l+1}^j + \theta k(U_{01} + \sigma h_l U_{11}) + O(k^2), \tag{3.9}$$

$$\bar{U}_{l-1}^j = \theta U_{l-1}^{j+1} + (1 - \theta)U_{l-1}^j = U_{l-1}^j + \theta k(U_{01} - h_l U_{11}) + O(k^2), \tag{3.10}$$

$$\bar{U}_{l+1/2}^j = \frac{1}{2}(\bar{U}_{l+1}^j + \bar{U}_l^j) = U_{l+1/2}^j + \theta k U_{01} + \frac{\sigma h_l^2}{8} U_{20} + O(kh_l + h_l^3 + k^2), \tag{3.11}$$

$$\bar{U}_{l-1/2}^j = \frac{1}{2}(\bar{U}_{l-1}^j + \bar{U}_l^j) = U_{l-1/2}^j + \theta k U_{01} + \frac{h_l^2}{8} U_{20} + O(kh_l + h_l^3 + k^2), \tag{3.12}$$

$$\bar{U}_{ul}^j = \frac{1}{k}(U_l^{j+1} - U_l^j) = U_{01} + \frac{k}{2} U_{02} + O(k^2), \tag{3.13}$$

$$\bar{U}_{ul+1}^j = \frac{1}{k}(U_{l+1}^{j+1} - U_{l+1}^j) = U_{ul+1}^j + \frac{k}{2} U_{02} + O(kh_l + k^2), \tag{3.14}$$

$$\bar{U}_{ul-1}^j = \frac{1}{k}(U_{l-1}^{j+1} - U_{l-1}^j) = U_{ul-1}^j + \frac{k}{2} U_{02} + O(kh_l + k^2), \tag{3.15}$$

$$\begin{aligned} \bar{U}_{ul+1/2}^j &= \frac{1}{2k}(U_{l+1}^{j+1} + U_l^{j+1} - U_{l+1}^j - U_l^j) \\ &= U_{ul+1/2}^j + \frac{k}{2} U_{02} + \frac{\sigma^2 h_l^2}{8} U_{21} + O(kh_l + h_l^3 + k^2), \end{aligned} \tag{3.16}$$

$$\begin{aligned} \bar{U}_{ul-1/2}^j &= \frac{1}{2k}(U_{l-1}^{j+1} + U_l^{j+1} - U_{l-1}^j - U_l^j) \\ &= U_{ul-1/2}^j + \frac{k}{2} U_{02} + \frac{h_l^2}{8} U_{21} + O(kh_l + h_l^3 + k^2), \end{aligned} \tag{3.17}$$

$$\bar{U}_{xl}^j = \frac{\bar{U}_{l+1}^j - (1 - \sigma^2)\bar{U}_l^j - \sigma^2\bar{U}_{l-1}^j}{h_l\sigma(\sigma + 1)} = U_{10} + \frac{1}{6}\sigma h_l^2 U_{30} + \theta k U_{11} + O(kh_l + h_l^3), \tag{3.18}$$

$$\bar{U}_{xl+1/2}^j = \frac{\bar{U}_{l+1}^j - \bar{U}_l^j}{\sigma h_l} = U_{xl+1/2}^j + \frac{1}{24}\sigma^2 h_l^2 U_{30} + \theta k U_{11} + O(kh_l + k^2 + h_l^3), \tag{3.19}$$

$$\bar{U}_{xl-1/2}^j = \frac{\bar{U}_l^j - \bar{U}_{l-1}^j}{h_l} = U_{xl-1/2}^j + \frac{1}{24}h_l^2 U_{30} + \theta k U_{11} + O(kh_l + k^2 + h_l^3), \tag{3.20}$$

$$\begin{aligned} \bar{U}_{xxl}^j &= \frac{2[\bar{U}_{l+1}^j - (1 + \sigma)\bar{U}_l^j + \sigma\bar{U}_{l-1}^j]}{\sigma(\sigma + 1)h_l^2} \\ &= U_{xxl}^j + \theta k U_{21} + \frac{(\sigma - 1)h_l}{3} U_{30} + O(k^2 + h_l^2), \end{aligned} \tag{3.21}$$

where ‘ θ ’ is a parameter to be determined.

With the help of the approximations (3.7)-(3.21), we can simplify the following approximations:

$$\begin{aligned} \bar{M}_l^j &= f(x_l, \bar{t}_j, \bar{U}_l^j, \bar{U}_{xl}^j, \bar{U}_{tl}^j) \\ &= M_l^j + \theta k(\delta_l^j + U_{01}\alpha_l^j + U_{11}\beta_l^j) + \frac{\sigma^2 h_l^2}{6} U_{30}\beta_l^j \\ &\quad + \frac{k}{2} U_{02}\gamma_l^j + O(kh_l + h_l^3 + k^2), \end{aligned} \tag{3.22}$$

$$\begin{aligned} \bar{M}_{l+1/2}^j &= f(x_{l+1/2}, \bar{t}_j, \bar{U}_{l+1/2}^j, \bar{U}_{xl+1/2}^j, \bar{U}_{tl+1/2}^j) \\ &= M_{l+1/2}^j + \theta k(\delta_l^j + U_{01}\alpha_l^j + U_{11}\beta_l^j) + \frac{\sigma^2 h_l^2}{24} (3U_{20}\alpha_l^j + U_{30}\beta_l^j + 3U_{21}\gamma_l^j) \\ &\quad + \frac{k}{2} U_{02}\gamma_l^j + O(kh_l + h_l^3 + k^2), \end{aligned} \tag{3.23}$$

$$\begin{aligned} \bar{M}_{l-1/2}^j &= f(x_{l-1/2}, \bar{t}_j, \bar{U}_{l-1/2}^j, \bar{U}_{xl-1/2}^j, \bar{U}_{tl-1/2}^j) \\ &= M_{l-1/2}^j + \theta k(\delta_l^j + U_{01}\alpha_l^j + U_{11}\beta_l^j) + \frac{h_l^2}{24} (3U_{20}\alpha_l^j + U_{30}\beta_l^j + 3U_{21}\gamma_l^j) \\ &\quad + \frac{k}{2} U_{02}\gamma_l^j + O(kh_l + h_l^3 + k^2). \end{aligned} \tag{3.24}$$

From the properties of spline function given by (2.16) and (2.17), we define the approximations:

$$\hat{U}_{xl-1/2}^j = \frac{\bar{U}_l^j - \bar{U}_{l-1}^j}{h_l} - \frac{h_l}{4} (2\beta_{2l}\bar{M}_l^j - \gamma_l\bar{M}_{l-1/2}^j), \tag{3.25}$$

$$\hat{U}_{xl+1/2}^j = \frac{\bar{U}_{l+1}^j - \bar{U}_l^j}{\sigma h_l} + \frac{h_l}{4} (2\beta_{1l}\bar{M}_l^j - \alpha_l\bar{M}_{l+1/2}^j). \tag{3.26}$$

With the help of the approximations (3.8)-(3.10), (3.22)-(3.24), and simplifying (3.25) and (3.26), we obtain

$$\hat{U}_{xl-1/2}^j = U_{xl-1/2}^j + \theta k U_{11} + O(k^2 + kh_l + h_l^3), \tag{3.27}$$

$$\hat{U}_{xl+1/2}^j = U_{xl+1/2}^j + \theta k U_{11} + O(k^2 + kh_l + h_l^3). \tag{3.28}$$

Now, we need $O(kh_l + h_l^3 + k^2)$ -approximations for U_l^j, U_{xl}^j and $O(k^2 + h_l^3)$ -approximation for \bar{U}_{tl}^j . Let

$$\hat{U}_l^j = \bar{U}_l^j + ah_l^2 \bar{U}_{xxl}^j, \tag{3.29}$$

$$\hat{U}_{xl}^j = \bar{U}_{xl}^j + bh_l(\bar{M}_{l+1/2}^j - \bar{M}_{l-1/2}^j), \tag{3.30}$$

$$\hat{U}_{tl}^j = \bar{U}_{tl}^j + c(\bar{U}_{tl+1}^j - (1 + \sigma)\bar{U}_{tl}^j + \sigma\bar{U}_{tl-1}^j), \tag{3.31}$$

where ‘a’, ‘b’ and ‘c’ are parameters to be determined.

With the help of the approximation (3.18), (3.23), (3.24), from (3.30) we obtain

$$\hat{U}_{xl}^j = U_{xl}^j + \theta k U_{11} + \frac{h_l^2}{6} [\sigma + 3b(1 + \sigma)] U_{30} + O(k^2 + kh_l + h_l^3), \quad \sigma \neq 1. \tag{3.32}$$

Equating the coefficient of h_l^2 to zero in equation (3.32), we obtain $b = \frac{-\sigma}{3(1+\sigma)}$ and equation (3.32) reduces to

$$\hat{U}_{xl}^j = U_{xl}^j + \theta k U_{11} + O(k^2 + kh_l + h_l^3), \quad \sigma_l \neq 1. \tag{3.33}$$

Similarly, simplifying (3.29) and (3.31), we obtain

$$\hat{U}_l^j = U_l^j + \theta k U_{01} + ah_l^2 U_{20} + O(k^2 + kh_l^2 + h_l^3), \tag{3.34}$$

$$\hat{U}_{tl}^j = U_{tl}^j + \frac{k}{2} U_{02} + c\sigma(1 + \sigma) \frac{h_l^2}{2} U_{21} + O(k^2 + h_l^3), \quad \sigma \neq 1. \tag{3.35}$$

Further, we define

$$\hat{M}_l^j = f(x_l, \bar{t}_j, \hat{U}_l^j, \hat{U}_{xl}^j, \hat{U}_{tl}^j), \tag{3.36}$$

$$\hat{M}_{l\pm 1/2}^j = f(x_{l\pm 1/2}, \bar{t}_j, \bar{U}_{l\pm 1/2}^j, \hat{U}_{xl\pm 1/2}^j, \bar{U}_{tl\pm 1/2}^j). \tag{3.37}$$

With the help of the approximations (3.7), (3.11)-(3.12), (3.16)-(3.17), (3.33)-(3.35), from (3.36)-(3.37), we obtain

$$\begin{aligned} \hat{M}_l^j &= M_l^j + \theta k(\delta_l^j + U_{01}\alpha_l^j + U_{11}\beta_l^j) + \frac{k}{2} U_{02}\gamma_l^j \\ &\quad + \frac{h_l^2}{2} (2aU_{20}\alpha_l^j + c\sigma(1 + \sigma)U_{21}\gamma_l^j) + O(k^2 + kh_l + h_l^3), \end{aligned} \tag{3.38}$$

$$\begin{aligned} \hat{M}_{l+1/2}^j &= M_{l+1/2}^j + \theta k(\delta_l^j + U_{01}\alpha_l^j + U_{11}\beta_l^j) + \frac{k}{2} U_{02}\gamma_l^j \\ &\quad + \frac{\sigma^2 h_l^2}{8} (U_{20}\alpha_l^j + U_{21}\gamma_l^j) + O(k^2 + kh_l + h_l^3), \end{aligned} \tag{3.39}$$

$$\begin{aligned} \hat{M}_{l-1/2}^j &= M_{l-1/2}^j + \theta k(\delta_l^j + U_{01}\alpha_l^j + U_{11}\beta_l^j) + \frac{k}{2} U_{02}\gamma_l^j \\ &\quad + \frac{h_l^2}{8} (U_{20}\alpha_l^j + U_{21}\gamma_l^j) + O(k^2 + kh_l + h_l^3). \end{aligned} \tag{3.40}$$

Using the approximation (3.8)-(3.10), (3.38)-(3.40), from (3.6), we obtain

$$\begin{aligned} & (U_{tl+1}^j - (1 + \sigma)U_{tl}^j + \sigma U_{tl-1}^j) + O(kh_l^3 + h_l^5) \\ &= \frac{\sigma h_l^2}{3} \left[\sigma M_{l+1/2}^j + \frac{(1 + \sigma)}{2} M_l^j + M_{l-1/2}^j + \frac{3(1 + \sigma)}{2} \theta k(\delta_l^j + U_{01}\alpha_l^j + U_{11}\beta_l^j - U_{21}) \right] \end{aligned}$$

$$\begin{aligned}
 &+ \frac{3k(1 + \sigma)}{4} U_{02} \gamma_l^j \\
 &+ \frac{h_l^2}{8} \{ (1 + \sigma^3) + 4a(1 + \sigma) \} U_{20} \alpha_l^j \\
 &+ \frac{h_l^2}{8} \{ (1 + \sigma^3) + 2c\sigma(1 + \sigma)^2 \} U_{21} \gamma_l^j \Big] + \hat{T}_l^j.
 \end{aligned} \tag{3.41}$$

Now with the help of the consistency condition (2.12) and equation (3.2), and from (3.41), we obtain the local truncation error

$$\begin{aligned}
 \hat{T}_l^j = &\frac{-\sigma h_l^2}{3} \left[\frac{3(1 + \sigma)}{2} \left(\frac{1}{2} - \theta \right) k U_{02} \gamma_l^j + \frac{h_l^2}{8} \{ (1 + \sigma^3) + 4a(1 + \sigma) \} U_{20} \alpha_l^j \right. \\
 &\left. + \frac{h_l^2}{8} \{ (1 + \sigma^3) + 2c\sigma(1 + \sigma)^2 \} U_{21} \gamma_l^j \right] + O(kh_l^3 + h_l^5), \quad \sigma \neq 1.
 \end{aligned} \tag{3.42}$$

The proposed non-polynomial spline in compression method (3.6) to be of $O(kh_l + h_l^3)$, the coefficients of kh_l^2 and h_l^4 in (3.42) must be zero.

Thus we obtain $\theta = \frac{1}{2}$, $a = \frac{-(1-\sigma+\sigma^2)}{4}$, $c = \frac{-(1-\sigma+\sigma^2)}{2\sigma(1+\sigma)}$ and the local truncation error given by (3.42) reduces to $\hat{T}_l^j = O(kh_l^3 + h_l^5)$.

4 Method extended to a system of quasi-linear parabolic equations

We now extend our method to the system of quasi-linear parabolic PDEs of the form

$$\frac{\partial^2 \mathbf{u}}{\partial x^2} = \mathbf{F}, \tag{4.1}$$

where $\mathbf{u} = [u^{(1)}, u^{(2)}, \dots, u^{(n)}]^T$, $\mathbf{F} = [f^{(1)}, f^{(2)}, \dots, f^{(n)}]^T$, T denotes the transpose of the matrix.

Throughout this section, we consider

$$f^{(i)} = f^{(i)}(x, t, u^{(1)}, u^{(2)}, \dots, u^{(n)}, u_x^{(1)}, u_x^{(2)}, \dots, u_x^{(n)}, u_t^{(1)}, u_t^{(2)}, \dots, u_t^{(n)}), \quad i = 1(1)n.$$

The initial and boundary conditions are given by

$$u^{(i)}(x, 0) = u_0^{(i)}(x), \quad 0 \leq x \leq 1, \tag{4.2}$$

$$u^{(i)}(0, t) = g_0^{(i)}(t), \quad u^{(i)}(1, t) = g_1^{(i)}(t), \quad t > 0, \tag{4.3}$$

where we assume that the functions $u_0^{(i)}(x)$, $g_0^{(i)}(t)$, $g_1^{(i)}(t)$ are sufficiently smooth.

Let $U_l^{(i)j}$ and $u_l^{(i)j}$ be the exact and approximate solution of the i th PDE of the system (4.1) at each grid point (x_l, t_j) . At the grid point (x_l, t_j) , we define the following approximations:

$$\bar{t}_j = t_j + \frac{k}{2}, \tag{4.4}$$

$$\bar{U}_l^{(i)j} = \frac{1}{2} (U_l^{(i)j+1} + U_l^{(i)j}), \tag{4.5}$$

$$\bar{U}_{l+1}^{(i)j} = \frac{1}{2} (U_{l+1}^{(i)j+1} + U_{l+1}^{(i)j}), \tag{4.6}$$

$$\bar{u}_{l-1}^{(ij)} = \frac{1}{2}(u_{l-1}^{(i)j+1} + u_{l-1}^{(i)j}), \tag{4.7}$$

$$\bar{u}_{l+1/2}^{(ij)} = \frac{1}{2}(\bar{u}_{l+1}^{(ij)} + \bar{u}_l^{(ij)}), \tag{4.8}$$

$$\bar{u}_{l-1/2}^{(ij)} = \frac{1}{2}(\bar{u}_{l-1}^{(ij)} + \bar{u}_l^{(ij)}), \tag{4.9}$$

$$\bar{u}_{tl}^{(ij)} = \frac{u_l^{(i)j+1} - u_l^{(i)j}}{k}, \tag{4.10}$$

$$\bar{u}_{tl+1}^{(ij)} = \frac{u_{l+1}^{(i)j+1} - u_{l+1}^{(i)j}}{k}, \tag{4.11}$$

$$\bar{u}_{tl-1}^{(ij)} = \frac{u_{l-1}^{(i)j+1} - u_{l-1}^{(i)j}}{k}, \tag{4.12}$$

$$\bar{u}_{tl+1/2}^{(ij)} = \frac{\bar{u}_{tl+1}^{(ij)} + \bar{u}_{tl}^{(ij)}}{2}, \tag{4.13}$$

$$\bar{u}_{tl-1/2}^{(ij)} = \frac{\bar{u}_{tl-1}^{(ij)} + \bar{u}_{tl}^{(ij)}}{2}, \tag{4.14}$$

$$\bar{u}_{xl}^{(ij)} = \frac{\bar{u}_{l+1}^{(ij)} - (1 - \sigma^2)\bar{u}_l^{(ij)} - \sigma^2\bar{u}_{l-1}^{(ij)}}{h_l\sigma(\sigma + 1)}, \tag{4.15}$$

$$\bar{u}_{xl+1/2}^{(ij)} = \frac{\bar{u}_{l+1}^{(ij)} - \bar{u}_l^{(ij)}}{\sigma h_l}, \tag{4.16}$$

$$\bar{u}_{xl-1/2}^{(ij)} = \frac{\bar{u}_l^{(ij)} - \bar{u}_{l-1}^{(ij)}}{h_l}, \tag{4.17}$$

$$\bar{u}_{xxl}^{(ij)} = \frac{2[\bar{u}_{l+1}^{(ij)} - (1 + \sigma)\bar{u}_l^{(ij)} + \sigma\bar{u}_{l-1}^{(ij)}]}{\sigma(\sigma + 1)h_l^2}. \tag{4.18}$$

Further, we define

$$\bar{M}_l^{(ij)} = f^{(i)}(x_l, \bar{t}_j, \bar{u}_l^{(1)j}, \bar{u}_l^{(2)j}, \dots, \bar{u}_l^{(n)j}, \bar{u}_{xl}^{(1)j}, \bar{u}_{xl}^{(2)j}, \dots, \bar{u}_{xl}^{(n)j}, \bar{u}_{tl}^{(1)j}, \bar{u}_{tl}^{(2)j}, \dots, \bar{u}_{tl}^{(n)j}), \tag{4.19}$$

$$\bar{M}_{l\pm 1/2}^{(ij)} = f^{(i)}(x_{l\pm 1/2}, \bar{t}_j, \bar{u}_{l\pm 1/2}^{(1)j}, \bar{u}_{l\pm 1/2}^{(2)j}, \dots, \bar{u}_{l\pm 1/2}^{(n)j}, \bar{u}_{xl\pm 1/2}^{(1)j}, \bar{u}_{xl\pm 1/2}^{(2)j}, \dots, \bar{u}_{xl\pm 1/2}^{(n)j}, \bar{u}_{tl\pm 1/2}^{(1)j}, \bar{u}_{tl\pm 1/2}^{(2)j}, \dots, \bar{u}_{tl\pm 1/2}^{(n)j}), \tag{4.20}$$

$$\hat{u}_l^{(ij)} = \bar{u}_l^{(ij)} - \frac{(1 - \sigma + \sigma^2)h_l^2}{4}\bar{u}_{xxl}^{(ij)}, \tag{4.21}$$

$$\hat{u}_{xl}^{(ij)} = \bar{u}_{xl}^{(ij)} - \frac{\sigma h_l}{3(1 + \sigma)}(\bar{M}_{l+1/2}^{(ij)} - \bar{M}_{l-1/2}^{(ij)}), \tag{4.22}$$

$$\hat{u}_{xl+1/2}^{(ij)} = \frac{\bar{u}_{l+1}^{(ij)} - \bar{u}_l^{(ij)}}{\sigma h_l} + \frac{h_l}{4}(2\beta_{1l}\bar{M}_l^{(ij)} - \alpha_l\bar{M}_{l+1/2}^{(ij)}), \tag{4.23}$$

$$\hat{u}_{xl-1/2}^{(ij)} = \frac{\bar{u}_l^{(ij)} - \bar{u}_{l-1}^{(ij)}}{h_l} - \frac{h_l}{4}(2\beta_{2l}\bar{M}_l^{(ij)} - \gamma_l\bar{M}_{l-1/2}^{(ij)}), \tag{4.24}$$

$$\hat{u}_{tl}^{(ij)} = \bar{u}_{tl}^{(ij)} - \frac{(1 - \sigma + \sigma^2)}{2\sigma(1 + \sigma)}(\bar{u}_{tl+1}^{(ij)} - (1 + \sigma)\bar{u}_{tl}^{(ij)} + \sigma\bar{u}_{tl-1}^{(ij)}), \tag{4.25}$$

where the values of $\alpha_l, \beta_{1l}, \beta_{2l}$ and γ_l are already defined in Section 2.

Finally, let

$$\hat{M}_l^{(i)j} = f^{(i)}(x_l, \bar{t}_j, \hat{U}_l^{(1)j}, \hat{U}_l^{(2)j}, \dots, \hat{U}_l^{(n)j}, \hat{U}_{xl}^{(1)j}, \hat{U}_{xl}^{(2)j}, \dots, \hat{U}_{xl}^{(n)j}, \hat{U}_{tl}^{(1)j}, \hat{U}_{tl}^{(2)j}, \dots, \hat{U}_{tl}^{(n)j}), \tag{4.26}$$

$$\begin{aligned} \hat{M}_{l\pm 1/2}^{(i)j} = f^{(i)}(x_{l\pm 1/2}, \bar{t}_j, \bar{U}_{l\pm 1/2}^{(1)j}, \bar{U}_{l\pm 1/2}^{(2)j}, \dots, \bar{U}_{l\pm 1/2}^{(n)j}, \hat{U}_{xl\pm 1/2}^{(1)j}, \hat{U}_{xl\pm 1/2}^{(2)j}, \dots, \\ \hat{U}_{xl\pm 1/2}^{(n)j}, \bar{U}_{tl\pm 1/2}^{(1)j}, \bar{U}_{tl\pm 1/2}^{(2)j}, \dots, \bar{U}_{tl\pm 1/2}^{(n)j}). \end{aligned} \tag{4.27}$$

Then at each grid point (x_i, t_j) , each differential equation of the system (4.1) is discretized by

$$\begin{aligned} [\bar{U}_{l+1}^{(i)j} - (1 + \sigma)\bar{U}_l^{(i)j} + \sigma\bar{U}_{l-1}^{(i)j}] \\ = \frac{\sigma h_l^2}{3} \left[\sigma \hat{M}_{l+1/2}^{(i)j} + \frac{(1 + \sigma)}{2} \hat{M}_l^{(i)j} + \hat{M}_{l-1/2}^{(i)j} \right] + \hat{T}_l^{(i)j}, \quad i = 1(1)n, \end{aligned} \tag{4.28}$$

where $\hat{T}_l^{(i)j} = O(kh_l^3 + h_l^5)$, provided $\sigma \neq 1$.

5 Application and stability analysis

Now let us consider the one-dimensional Burgers equation in polar coordinates

$$\frac{1}{R_e} \left(u_{rr} + \frac{p}{r} u_r - \frac{p}{r^2} u \right) = u_t + uu_r + g(r, t), \quad 0 < r < 1, t > 0, \tag{5.1}$$

where $R_e > 0$ denotes the Reynolds number. For $p = 1$ and 2 , the above equation represents Burgers' equation in cylindrical and spherical coordinates, respectively. It is the simplest model for the differential equations of fluid flow. It is used in fluid dynamics as a simplified model for turbulence, boundary layer behavior and shock wave formation. The viscous Burgers equation in polar coordinates is a useful test equation for investigating various numerical schemes, which are then applied to more complicated systems of partial differential equations. It shows a structure roughly similar to that of Navier-Stokes equations due to the form of the nonlinear convection term and the occurrence of the viscosity term. So it can be considered as a simplified form of the one-space dimensional Navier-Stokes equation. If we suppress the variables θ, z and θ, φ from the Navier-Stokes equations of motion in cylindrical polar coordinates (r, θ, z, t) and spherical polar coordinates (r, θ, φ, t) , respectively (see [15]), we obtain Burgers' equation (5.1) in polar coordinates. The high-accuracy numerical solution of Burgers' equation in polar coordinates plays an important role for viscous fluid flow. It has been experienced in the past that the high-accuracy numerical solution usually deteriorates in the vicinity of the singular point say $r = 0$, whereas the proposed spline method is applicable to 1D nonlinear parabolic equations irrespective of coordinates, that is, the proposed spline method is directly applicable to solve equation (5.1). We do not require any modification in the spline scheme unlike other methods discussed in [16, 17]. Thus the numerical schemes for problems in polar coordinates are of importance in this discussion.

Re-write equation (5.1) as

$$\varepsilon u_{rr} = u_t + Q(r)u_r + uu_r + S(r)u + g(r, t), \tag{5.2}$$

where $R_e = \varepsilon^{-1} > 0$ represents a Reynolds number and $Q(r) = \frac{-p\varepsilon}{r}, S(r) = \frac{p\varepsilon}{r^2}$.

Replacing the variable ‘ x ’ by ‘ r ’ and applying the method (3.6) to the differential equation (5.2), we obtain

$$\varepsilon [\bar{U}_{l+1}^j - (1 + \sigma)\bar{U}_l^j + \sigma\bar{U}_{l-1}^j] = \frac{\sigma h_l^2}{3} \left[\sigma \hat{M}_{l+1/2}^j + \frac{(1 + \sigma)}{2} \hat{M}_l^j + \hat{M}_{l-1/2}^j \right] + \hat{T}_l^j, \tag{5.3}$$

where

$$\begin{aligned} \hat{M}_l^j &= \hat{U}_{tl}^j + Q_l \hat{U}_{rl}^j + \hat{U}_l^j \hat{U}_{rl}^j + S_l \hat{U}_l^j + \bar{g}_l^j, \\ \hat{M}_{l\pm 1/2}^j &= \bar{U}_{t\pm 1/2}^j + Q_{l\pm 1/2} \hat{U}_{r\pm 1/2}^j + \bar{U}_{l\pm 1/2}^j \hat{U}_{r\pm 1/2}^j + S_{l\pm 1/2} \bar{U}_{l\pm 1/2}^j + \bar{g}_{l\pm 1/2}^j, \end{aligned}$$

where $\bar{U}_{l\pm 1/2}^j$, $\bar{U}_{t\pm 1/2}^j$, \hat{U}_l^j , \hat{U}_{rl}^j , $\hat{U}_{r\pm 1/2}^j$ and \hat{U}_{tl}^j are defined in Section 3 and $Q_l = Q(r_l)$, $Q_{l\pm 1/2} = Q(r_{l\pm 1/2})$, $S_l = S(r_l)$, $S_{l\pm 1/2} = S(r_{l\pm 1/2})$, $\bar{g}_l = g(r_l, t_j + \frac{k}{2})$, $\bar{g}_{l\pm 1/2} = g(r_{l\pm 1/2}, t_j + \frac{k}{2})$.

Note that the scheme (5.3) is of $O(kh_l + h_l^3)$ for the solution of differential equation (5.1) and is free from the terms $1/(r_{l\pm 1})$, thus, it is very easily solved for $l = 1(1)N; j = 0, 1, 2, \dots$, in the solution region without any modification. We do not require any fictitious point to solve the singular problem.

For stability, we consider the 1-D linear parabolic equation with variable coefficients

$$v u_{xx} = u_t + D(x)u_x + f(x, t), \quad 0 < x < 1, t > 0, \tag{5.4}$$

where $v > 0$ and D and f are sufficiently smooth functions. Applying the method (3.6) to the differential equation (5.4) on a uniform mesh (that is, when $h_{l+1} = h_l = h$), we obtain the following scheme for the solution of the above differential equation:

$$v (\bar{U}_{l+1}^j - 2\bar{U}_l^j + \bar{U}_{l-1}^j) = \frac{h^2}{3} [\hat{M}_{l+1/2}^j + \hat{M}_{l-1/2}^j + \hat{M}_l^j] + \hat{T}_l^j, \tag{5.5}$$

where

$$\hat{M}_l^j = \hat{U}_{tl}^j + D_l \hat{U}_{xl}^j + \bar{f}_l^j, \tag{5.6}$$

$$\hat{M}_{l+1/2}^j = \bar{U}_{t+1/2}^j + D_{l+1/2} \hat{U}_{xl+1/2}^j + \bar{f}_{l+1/2}^j, \tag{5.7}$$

$$\hat{M}_{l-1/2}^j = \bar{U}_{t-1/2}^j + D_{l-1/2} \hat{U}_{xl-1/2}^j + \bar{f}_{l-1/2}^j, \tag{5.8}$$

where

$$\begin{aligned} \hat{U}_{xl-1/2}^j &= \frac{\bar{U}_l^j - \bar{U}_{l-1}^j}{h} - \frac{h}{4} (\bar{\beta} \bar{M}_l^j - \bar{\alpha} \bar{M}_{l-1/2}^j), \\ \hat{U}_{xl+1/2}^j &= \frac{\bar{U}_{l+1}^j - \bar{U}_l^j}{h} + \frac{h}{4} (\bar{\beta} \bar{M}_l^j - \bar{\alpha} \bar{M}_{l+1/2}^j), \\ \bar{\alpha} &= \frac{1}{2\mu^2} \left[\frac{\mu}{\sin \mu} - \cos \mu \right], \quad \bar{\beta} = \frac{1}{\mu^2} (1 - \mu \cot \mu) \end{aligned}$$

and $\bar{f}_l^j = f(x_l, t_j + \frac{k}{2}), \dots$

The approximations associated with (5.6)-(5.8) are already defined in Section 3. In order to discuss the stability, we require the following approximations:

$$D_{l\pm 1/2} = D_l \pm \frac{h}{2} D_{xl} + \frac{h^2}{8} D_{xxl} \pm O(h^3), \tag{5.9}$$

$$\bar{f}_{l\pm 1/2} = \bar{f} \pm \frac{h}{2} \bar{f}_x + \frac{h^2}{8} \bar{f}_{xx} \pm O(h^3), \tag{5.10}$$

$$\bar{\alpha} = \frac{1}{3} + O(h^2), \tag{5.11}$$

$$\bar{\beta} = \frac{1}{3} + O(h^2). \tag{5.12}$$

With the help of the approximations (5.6)-(5.8) and (5.9)-(5.12), neglecting higher-order terms, from (5.5), we obtain

$$\begin{aligned} \nu \delta_x^2 \bar{U}_l^j &= \frac{h^2}{12} \left[(12 + \delta_x^2) \bar{U}_{tl}^j - \frac{h D_l}{2\nu} (2\mu_x \delta_x) \bar{U}_{tl}^j \right] \\ &+ \frac{h^2}{12} \left[2D_{xl} - \frac{D_l^2}{\nu} \right] \delta_x^2 \bar{U}_l^j + \frac{h}{24} \left[12D_l + h^2 \left(D_{xxl} - \frac{D_l D_{xl}}{\nu} \right) \right] (2\mu_x \delta_x) \bar{U}_l^j \\ &+ \frac{h^2}{12} \left[12\bar{f}_l^j + h^2 \left(\bar{f}_{xxl}^j - \frac{D_l \bar{f}_{xl}^j}{\nu} \right) \right] + \hat{T}_l^j, \end{aligned} \tag{5.13}$$

where $\delta_x U_l^j = (U_{l+1/2}^j - U_{l-1/2}^j)$ and $\mu_x U_l^j = \frac{1}{2}(U_{l+1/2}^j + U_{l-1/2}^j)$.

Multiplying (5.13) throughout by $\lambda = (k/h^2)$ and neglecting the local truncation error term, we have

$$\begin{aligned} &\left[1 + \frac{1}{12} (1 - 6\lambda\nu + \lambda P_1) \delta_x^2 - \frac{1}{12} (hQ_2 - \lambda P_2) (2\mu_x \delta_x) \right] u_l^{j+1} \\ &= \left[1 + \frac{1}{12} (1 + 6\lambda\nu - \lambda P_1) \delta_x^2 - \frac{1}{12} (hQ_2 + \lambda P_2) (2\mu_x \delta_x) \right] u_l^j + FF, \end{aligned} \tag{5.14}$$

where

$$\begin{aligned} P_1 &= \frac{h^2}{2} \left[2D_{xl} - \frac{D_l^2}{\nu} \right], & P_2 &= \frac{h}{4} \left[12D_l + h^2 \left(D_{xxl} - \frac{D_l D_{xl}}{\nu} \right) \right], & Q_2 &= \frac{D_l}{2\nu}, \\ FF &= \frac{-k}{12} \left[12\bar{f}_l^j + h^2 \left(\bar{f}_{xxl}^j - \frac{D_l \bar{f}_{xl}^j}{\nu} \right) \right]. \end{aligned}$$

To study the stability of scheme (5.14), we apply the von Neumann linear stability analysis. Let $\varepsilon_l^j = \xi^j e^{i\eta l}$ be the error at the grid point (x_l, t_j) , where ξ is a complex number and η is a real number. Substituting $\varepsilon_l^j = \xi^j e^{i\eta l}$ into the homogeneous part of the error equation of (5.14), we obtain the amplification factor ξ as

$$\begin{aligned} \xi &= \frac{(1 - \frac{1}{3}(1 + 6\lambda\nu - \lambda P_1) \sin^2 \frac{\eta}{2} - \frac{i}{6}(hQ_2 + \lambda P_2) \sin \eta)}{(1 - \frac{1}{3}(1 - 6\lambda\nu + \lambda P_1) \sin^2 \frac{\eta}{2} - \frac{i}{6}(hQ_2 - \lambda P_2) \sin \eta)} \\ &= \frac{1 + (X + iY)}{1 - (X + iY)}, \end{aligned} \tag{5.15}$$

where

$$X = \frac{-\lambda \left[\left(\frac{1}{3}(6\nu - P_1) \sin^2 \frac{\eta}{2} \right) \left(1 - \frac{1}{3} \sin^2 \frac{\eta}{2} \right) - \frac{h}{36} P_2 Q_2 \sin^2 \eta \right]}{\left(1 - \frac{1}{3} \sin^2 \frac{\eta}{2} \right)^2 + \frac{h^2}{36} Q_2^2 \sin^2 \eta}.$$

For stability, it is required that $|\xi|^2 \leq 1$. Imposing this condition on (5.15), we get

$$\begin{aligned} \left| \frac{1 + (X + iY)}{1 - (X + iY)} \right|^2 &\leq 1 \\ \Rightarrow (1 + X)^2 + Y^2 &\leq (1 - X)^2 + Y^2 \\ \Rightarrow X &\leq 0. \end{aligned}$$

Above inequality is satisfied for all values of η and, $D(x) = \frac{-\alpha v}{x}$, $\alpha = 1$ and 2 . Hence the scheme (5.14) is unconditionally stable.

Next, we consider the fourth-order parabolic equations

$$\left(\varepsilon \frac{\partial^2}{\partial x^2} - \frac{\partial}{\partial t} \right)^2 u \equiv \varepsilon^2 \frac{\partial^4 u}{\partial x^4} - 2\varepsilon \frac{\partial^3 u}{\partial x^2 \partial t} + \frac{\partial^2 u}{\partial t^2} = f(x, t), \quad 0 < x < 1, t > 0, \tag{5.16}$$

where $\varepsilon > 0$ and f is sufficiently smooth function.

The initial values of u, u_t are prescribed at $t = 0$ and boundary values of u, u_{xx} are prescribed at $x = 0$ and $x = 1$. Since the grid lines are parallel to the coordinate axes and the values of u, u_{xx} are exactly known on the boundary, the values of successive tangential partial derivatives of u, u_{xx} , i.e., the values of u_t, u_{xxt}, \dots , are also known on the boundary $x = 0$ and $x = 1$. Similarly, the values of $u_x, u_{xx}, u_{tx}, \dots$ are also known at $t = 0$. Hence the values of $u_{xx}(x, 0) - u_t(x, 0), u_{xx}(0, t) - u_t(0, t)$ and $u_{xx}(1, t) - u_t(1, t)$ are known exactly on the boundary.

Now, equation (5.16) can be re-written as

$$\varepsilon u_{xx} = u_t + v, \tag{5.17a}$$

$$\varepsilon v_{xx} = v_t + f(x, t). \tag{5.17b}$$

Applying the numerical method (4.28) to the above system of equations and neglecting local truncation errors, we obtain the following non-polynomial spline in compression schemes in coupled form:

$$\varepsilon (\bar{u}_{l+1}^j - 2\bar{u}_l^j + \bar{u}_{l-1}^j) = \frac{h^2}{3} [\bar{u}_{l+\frac{1}{2}}^j + \bar{u}_{l-\frac{1}{2}}^j + \hat{u}_{l,l}^j + \bar{v}_{l+\frac{1}{2}}^j + \bar{v}_{l-\frac{1}{2}}^j + \hat{v}_l^j], \tag{5.18a}$$

$$\varepsilon (\bar{v}_{l+1}^j - 2\bar{v}_l^j + \bar{v}_{l-1}^j) = \frac{h^2}{3} [\bar{v}_{l+\frac{1}{2}}^j + \bar{v}_{l-\frac{1}{2}}^j + \hat{v}_{l,l}^j] + \frac{h^2}{3} [\bar{f}_{l+1/2}^j + \bar{f}_{l-1/2}^j + \bar{f}_l^j]. \tag{5.18b}$$

Using the approximations defined in Section 4, and multiplying (5.18a) and (5.18b) throughout by $\lambda = (k/h^2)$, we get

$$\begin{aligned} 6\lambda\varepsilon\delta_x^2(u_l^{j+1} + u_l^j) &= [(u_{l+1}^{j+1} + 10u_l^{j+1} + u_{l-1}^{j+1}) - (u_{l+1}^j + 10u_l^j + u_{l-1}^j)] \\ &\quad + \frac{k}{2}(v_{l+1}^{j+1} + 10v_l^{j+1} + v_{l-1}^{j+1}) + \frac{k}{2}(v_{l+1}^j + 10v_l^j + v_{l-1}^j), \end{aligned} \tag{5.19a}$$

$$\begin{aligned} 6\lambda\varepsilon\delta_x^2(v_l^{j+1} + v_l^j) &= [(v_{l+1}^{j+1} + 10v_l^{j+1} + v_{l-1}^{j+1}) - (v_{l+1}^j + 10v_l^j + v_{l-1}^j)] \\ &\quad + 4k[\bar{f}_{l+1/2}^j + \bar{f}_{l-1/2}^j + \bar{f}_l^j]. \end{aligned} \tag{5.19b}$$

Neglecting the homogeneous part, the above system in matrix form may be written as

$$\begin{bmatrix} \mathbf{A}_{11} & \mathbf{A}_{12} \\ \mathbf{0} & \mathbf{A}_{11} \end{bmatrix} \begin{bmatrix} \mathbf{u}^{j+1} \\ \mathbf{v}^{j+1} \end{bmatrix} = \begin{bmatrix} \mathbf{B}_{11} & \mathbf{B}_{12} \\ \mathbf{0} & \mathbf{B}_{11} \end{bmatrix} \begin{bmatrix} \mathbf{u}^j \\ \mathbf{v}^j \end{bmatrix},$$

or

$$\mathbf{A}\mathbf{Y}^{j+1} = \mathbf{B}\mathbf{Y}^j, \tag{5.20}$$

where \mathbf{A}_{ij} and \mathbf{B}_{ij} , $i, j = 1, 2$ are $N \times N$ tri-diagonal matrices are given by

$$\begin{aligned} \mathbf{A}_{11} &= [1, 10, 1] - 6\lambda\varepsilon[1, -2, 1], & \mathbf{A}_{12} &= \frac{k}{2}[1, 10, 1], \\ \mathbf{B}_{11} &= [1, 10, 1] + 6\lambda\varepsilon[1, -2, 1], & \mathbf{B}_{12} &= -\frac{k}{2}[1, 10, 1], \end{aligned}$$

and

$$\mathbf{A} = \begin{bmatrix} \mathbf{A}_{11} & \mathbf{A}_{12} \\ \mathbf{0} & \mathbf{A}_{11} \end{bmatrix}, \quad \mathbf{B} = \begin{bmatrix} \mathbf{B}_{11} & \mathbf{B}_{12} \\ \mathbf{0} & \mathbf{B}_{11} \end{bmatrix}, \quad \mathbf{Y}^j = \begin{bmatrix} \mathbf{u}^j \\ \mathbf{v}^j \end{bmatrix}, \quad \mathbf{Y}^{j+1} = \begin{bmatrix} \mathbf{u}^{j+1} \\ \mathbf{v}^{j+1} \end{bmatrix}.$$

Assume that the matrix \mathbf{A} is non-singular. Pre-multiplying both sides of (5.20) by \mathbf{A}^{-1} , we get

$$\mathbf{Y}^{j+1} = \mathbf{A}^{-1}\mathbf{B}\mathbf{Y}^j. \tag{5.21}$$

The eigenvalues of $N \times N$ tri-diagonal matrix $[a, b, c]$ are defined by

$$\begin{aligned} \lambda_s &= b + 2\sqrt{ac} \cos \frac{s\pi}{N+1} = b + 2\sqrt{ac}(1 - 2\sin^2 \psi), \\ 2\psi &= \frac{s\pi}{N+1}, \quad s = 1(1)N. \end{aligned} \tag{5.22}$$

Using equation (5.22), the eigenvalues of the tri-diagonal matrices \mathbf{A}_{11} , \mathbf{A}_{12} , \mathbf{B}_{11} and \mathbf{B}_{12} are given by

$$\begin{aligned} 12 - 4\sin^2 \psi + 24\lambda\varepsilon \sin^2 \psi, & \quad \frac{k}{2}[12 - 4\sin^2 \psi], \\ 12 - 4\sin^2 \psi - 24\lambda\varepsilon \sin^2 \psi & \quad \text{and} \quad -\frac{k}{2}[12 - 4\sin^2 \psi], \end{aligned}$$

respectively.

The characteristic equations of the matrices \mathbf{A} and \mathbf{B} are given by

$$\begin{vmatrix} 12 - 4\sin^2 \psi + 24\lambda\varepsilon \sin^2 \psi - \xi & \frac{k}{2}[12 - 4\sin^2 \psi] \\ 0 & 12 - 4\sin^2 \psi + 24\lambda\varepsilon \sin^2 \psi - \xi \end{vmatrix} = 0, \tag{5.23}$$

and

$$\begin{vmatrix} 12 - 4\sin^2 \psi - 24\lambda\varepsilon \sin^2 \psi - \eta & \frac{k}{2}[12 - 4\sin^2 \psi] \\ 0 & 12 - 4\sin^2 \psi - 24\lambda\varepsilon \sin^2 \psi - \eta \end{vmatrix} = 0, \tag{5.24}$$

respectively. Hence the eigenvalues of **A** are given by $\xi = 12 - 4 \sin^2 \psi + 24\lambda\varepsilon \sin^2 \psi$, and the eigenvalues of **B** are given by $\eta = 12 - 4 \sin^2 \psi - 24\lambda\varepsilon \sin^2 \psi$.

Since **A**⁻¹ and **B** commute with each other, the eigenvalues of **A**⁻¹**B** are given by

$$\rho = \frac{12 - 4 \sin^2 \psi - 24\lambda\varepsilon \sin^2 \psi}{12 - 4 \sin^2 \psi + 24\lambda\varepsilon \sin^2 \psi}. \tag{5.25}$$

For stability, it is required that $|\rho| \leq 1$ for all values of ψ . Imposing this condition on (5.25) yields

$$-1 \leq \frac{12 - 4 \sin^2 \psi - 24\lambda\varepsilon \sin^2 \psi}{12 - 4 \sin^2 \psi + 24\lambda\varepsilon \sin^2 \psi} \leq 1. \tag{5.26}$$

Both inequalities of (5.26) are true for all values of ψ . Hence the scheme (5.19a)-(5.19b) is unconditionally stable.

6 Numerical illustrations

In this section, we have solved several benchmark problems using the proposed method based on spline in compression and compared the results with the results obtained by other researchers. The exact solutions are provided in each case. The right hand side homogeneous functions, initial and boundary conditions are obtained using the exact solution as a test procedure. The linear equations are solved using a tri-diagonal solver, whereas nonlinear equations are solved using the Newton-Raphson method. While using the Newton-Raphson method, we choose **0** as the initial guess. All the computations are carried out using MATLAB codes.

From equation (2.13), we have obtained the value $\mu_l = \mu_{l+1} = 8.986818916$. In order to compute the proposed method (3.6), we have evaluated the values of

$$\alpha_l = \frac{\sigma}{2\mu_{l+1}^2} \left[\frac{\mu_{l+1}}{\sin \mu_{l+1}} - \cos \mu_{l+1} \right], \quad \beta_{1l} = \frac{\sigma}{2\mu_{l+1}^2} [1 - \mu_{l+1} \cot \mu_{l+1}],$$

$$\beta_{2l} = \frac{1}{2\mu_l^2} [1 - \mu_l \cot \mu_l] \quad \text{and} \quad \gamma_l = \frac{1}{2\mu_l^2} \left[\frac{\mu_l}{\sin \mu_l} - \cos \mu_l \right]$$

using the values of μ_l and μ_{l+1} .

The given interval $[0, 1]$ is divided into $(N + 1)$ parts with $0 = x_0 < x_1 < \dots < x_N < x_{N+1} = 1$, where $h_l = x_l - x_{l-1}$, $l = 1, 2, \dots, N + 1$ and $\sigma = h_{l+1}/h_l > 0$, $l = 1, 2, \dots, N$.

We can write

$$1 = x_{N+1} - x_0 = (x_{N+1} - x_N) + (x_N - x_{N-1}) + \dots + (x_1 - x_0)$$

$$= h_{N+1} + h_N + \dots + h_1 = (\sigma^N + \sigma^{N-1} + \dots + \sigma^2 + \sigma)h_1. \tag{6.1}$$

Thus,

$$h_1 = 1/(\sigma + \sigma^2 + \dots + \sigma^N). \tag{6.2}$$

Alternatively, (6.2) can be re-written as

$$h_1 = (1 - \sigma)/(1 - \sigma^{N+1}). \tag{6.3}$$

By prescribing the total number of mesh points $(N + 2)$, we can compute the value of h_1 from (6.2) or (6.3). This is the first mesh spacing on the left and remaining mesh is determined by $h_{l+1} = \sigma h_l, l = 1, 2, \dots, N$.

Example 1 The one-dimensional GBFE is given by the following form:

$$\varepsilon u_{xx} = u_t + \alpha u^\delta u_x + \beta u(u^\delta - 1), \quad a \leq x \leq b, t > 0, \tag{6.4}$$

where the real valued function $u = u(x, t)$ is a sufficiently smooth function of the space and time variables; $[a, b] = [0, 1]$, and α, β are real parameters and δ is a positive integer.

The initial condition associated with differential equation (6.4) is given by

$$u(x, 0) = \left[\frac{\gamma}{2} + \frac{\gamma}{2} \tanh(a_1 x) \right]^{\frac{1}{\delta}}, \quad a \leq x \leq b, \tag{6.5}$$

and the boundary conditions associated with (6.4) are given by

$$u(a, t) = \left[\frac{\gamma}{2} + \frac{\gamma}{2} \tanh(a_1(a - a_2 t)) \right]^{\frac{1}{\delta}}, \quad t \geq 0, \tag{6.6}$$

$$u(b, t) = \left[\frac{\gamma}{2} + \frac{\gamma}{2} \tanh(a_1(b - a_2 t)) \right]^{\frac{1}{\delta}}, \quad t \geq 0. \tag{6.7}$$

The exact solution [6] of (6.4) is given by

$$u(x, t) = \left[\frac{\gamma}{2} + \frac{\gamma}{2} \tanh(a_1(x - a_2 t)) \right]^{\frac{1}{\delta}}, \quad t \geq 0, \tag{6.8}$$

where

$$\varepsilon = 1, \quad a_1 = \frac{-\alpha \delta}{2(1 + \delta)}, \quad a_2 = \frac{\alpha}{(1 + \delta)} + \frac{\beta(1 + \delta)}{\alpha}.$$

This problem is solved with $N = 10, 16, k = 0.0001$ and mesh ratio $\sigma = 0.9$ by present method. The following cases have been discussed for different values of the parameters α, β, γ and δ , which are involved in equation (6.4).

Case 1.1: We choose $\alpha = 0.001, \beta = 0.001$.

Case 1.1(a): In this case, results are computed for different time levels and $\delta = 1, 4$. The maximum absolute errors are tabulated for $x = 0.1, 0.5, 0.9$ in Tables 1-2.

Case 1.1(b): In this case, results are computed for different time levels and $\delta = 1, 4, 8$. The maximum absolute errors are tabulated for $t = 1, 2, 3, 4, 5$ in Table 3.

Case 1.2: We consider $\alpha = 1, \beta = 1, N = 10$. In this case, results are computed for different time levels $t = 0.2, 0.4, 0.6, 0.8, 1.0$ and $\delta = 1, 2, 4$. The maximum absolute errors are tabulated in Tables 4-6.

Case 1.3: We consider $\alpha = 1, \beta = 0, N = 10$. In this case, results are computed for different time levels and $\delta = 1, 2, 8$. The maximum absolute errors are tabulated for $x = 0.1, 0.5, 0.9$ in Tables 7-9.

Table 1 Example 1: Case 1.1(a)(i): Maximum absolute errors at $\delta = 1$

x	t	Method given in [23]	Method given in [5]	Proposed method (3.6)
0.1	0.001	1.11(-16)	5.55(-16)	5.55(-17)
	0.005	9.43(-16)	1.77(-15)	7.77(-16)
	0.010	4.21(-15)	2.55(-15)	3.13(-14)
0.5	0.001	1.11(-16)	3.88(-16)	1.66(-16)
	0.005	4.44(-16)	2.60(-15)	1.38(-15)
	0.010	1.66(-16)	4.99(-15)	8.16(-15)
0.9	0.001	0	1.05(-15)	5.55(-17)
	0.005	1.99(-15)	3.44(-15)	0
	0.010	5.05(-15)	5.16(-15)	4.44(-16)

Table 2 Example 1: Case 1.1 (a)(ii): Maximum absolute errors at $\delta = 4$

x	t	Method given in [23]	Method given in [5]	Proposed method (3.6)
0.1	0.001	1.11(-16)	3.76(-14)	1.11(-16)
	0.005	2.22(-16)	1.43(-13)	9.99(-16)
	0.010	6.66(-16)	2.39(-13)	1.75(-16)
0.5	0.001	1.12(-16)	3.20(-14)	1.11(-16)
	0.005	3.33(-16)	1.61(-13)	3.33(-16)
	0.010	3.33(-16)	3.22(-13)	2.88(-15)
0.9	0.001	1.11(-16)	3.84(-14)	1.11(-16)
	0.005	5.55(-16)	1.45(-13)	1.11(-16)
	0.010	1.11(-15)	2.41(-13)	2.22(-16)

Table 3 Example 1: Case 1.1(b): Maximum absolute errors

t	$\delta = 1$	$\delta = 4$	$\delta = 8$
1.0	3.44(-15)	9.95(-14)	9.55(-13)
2.0	1.66(-15)	9.61(-14)	9.54(-13)
3.0	1.33(-15)	9.73(-14)	9.61(-13)
4.0	1.31(-15)	9.76(-14)	9.88(-13)
5.0	1.22(-15)	9.78(-14)	9.89(-13)

Table 4 Example 1: Case 1.2(a): Maximum absolute errors at $\delta = 1$

t	Method given in [24]	Method given in [5]	Proposed method (3.6)
0.2	5.5574(-07)	3.5315(-07)	3.4453(-09)
0.4	9.0550(-07)	1.7573(-07)	2.9736(-09)
0.6	2.1880(-06)	1.2889(-07)	2.1401(-09)
0.8	2.9331(-06)	3.8543(-07)	1.5383(-09)
1.0	3.0145(-06)	6.1749(-07)	1.2262(-09)

Table 5 Example 1: Case 1.2(b): Maximum absolute errors at $\delta = 2$

t	Method given in [24]	Method given in [5]	Proposed method (3.6)
0.2	2.5610(-06)	7.9688(-07)	2.9321(-07)
0.4	4.2430(-06)	1.4540(-06)	3.9463(-07)
0.6	3.5684(-06)	1.8274(-06)	3.7075(-07)
0.8	1.4651(-06)	1.8775(-06)	2.7398(-07)
1.0	5.5423(-06)	1.6771(-06)	1.7040(-07)

Table 6 Example 1: Case 1.2(c): Maximum absolute errors at $\delta = 4$

t	Method given in [24]	Method given in [5]	Proposed method (3.6)
0.2	1.7616(-06)	3.2650(-06)	5.0521(-07)
0.4	4.1735(-07)	3.5607(-06)	3.8995(-07)
0.6	2.4240(-06)	2.5228(-06)	1.6247(-07)
0.8	2.3575(-06)	1.4074(-06)	4.6672(-08)
1.0	1.4435(-06)	6.9013(-07)	1.0805(-08)

Table 7 Example 1: Case 1.3(a): Maximum absolute errors at $\delta = 1$

x	t	Method given in [25]	Method given in [5]	Proposed method (3.6)
0.1	0.5	1.68(-11)	2.59(-12)	5.66(-13)
	1.0	1.79(-11)	2.74(-12)	3.42(-13)
	2.0	1.46(-11)	2.74(-12)	6.27(-13)
0.5	0.5	3.40(-12)	7.36(-13)	7.52(-14)
	1.0	3.72(-12)	7.99(-13)	4.81(-14)
	2.0	3.13(-12)	8.39(-13)	3.06(-14)
0.9	0.5	1.31(-11)	2.67(-12)	5.55(-17)
	1.0	1.37(-11)	2.96(-12)	5.55(-17)
	2.0	1.07(-11)	3.24(-12)	8.88(-16)

Table 8 Example 1: Case 1.3(b): Maximum absolute errors at $\delta = 2$

x	t	Method given in [25]	Method given in [5]	Proposed method (3.6)
0.1	0.5	4.49(-11)	2.83(-11)	6.14(-12)
	1.0	4.19(-11)	2.78(-11)	7.28(-12)
	2.0	2.70(-11)	2.41(-11)	9.17(-12)
0.5	0.5	8.13(-12)	8.42(-12)	2.24(-13)
	1.0	7.72(-12)	8.50(-12)	2.71(-13)
	2.0	4.77(-12)	7.85(-12)	3.55(-13)
0.9	0.5	3.55(-11)	3.13(-11)	3.33(-16)
	1.0	3.23(-11)	3.23(-11)	3.33(-16)
	2.0	1.98(-11)	3.14(-11)	4.44(-16)

Table 9 Example 4: Case 1.3(c): Maximum absolute errors at $\delta = 8$.

x	t	Method given in [25]	Method given in [5]	Proposed method (3.6)
0.1	0.5	4.60(-11)	9.37(-12)	1.20(-11)
	1.0	4.39(-11)	8.93(-12)	1.25(-11)
	2.0	3.78(-11)	7.72(-12)	1.31(-11)
0.5	0.5	7.03(-12)	3.06(-12)	4.36(-13)
	1.0	6.75(-12)	2.99(-12)	4.57(-13)
	2.0	5.67(-12)	2.74(-12)	4.88(-13)
0.9	0.5	3.69(-11)	1.19(-11)	5.55(-16)
	1.0	3.45(-11)	1.18(-11)	6.66(-16)
	2.0	2.84(-11)	1.13(-11)	6.66(-16)

Example 2 Consider equation (6.4) with $\alpha = 1, \beta = 0, \delta = 1$ initial and boundary conditions as given in Mittal and Jiwari [18], namely

$$u(x, 0) = x(1 - x^2), \quad 0 < x < 1, \tag{6.9a}$$

$$u(0, t) = u(1, t) = 0, \quad t > 0. \tag{6.9b}$$

In this example, we have computed solutions for $\varepsilon = 2^{-3}$ and 2^{-9} at $t = 0.1, 0.3, 0.6, 0.9$ with step size $k = 0.001$ and mesh ratio $\sigma = 0.9$. The computed numerical solutions as presented in Figure 1(a)-(b) are consistent with the dynamics of the corresponding differential equations. Similar patterns have been presented in [8, 18, 19] also.

Example 3 Consider equation (6.4) with $\alpha = 0, \delta = 1$ initial and boundary conditions as given in Zhao *et al.* [20], namely

$$u(x, 0) = x(1 - x^2)e^x, \quad -1 \leq x \leq 1, \tag{6.10a}$$

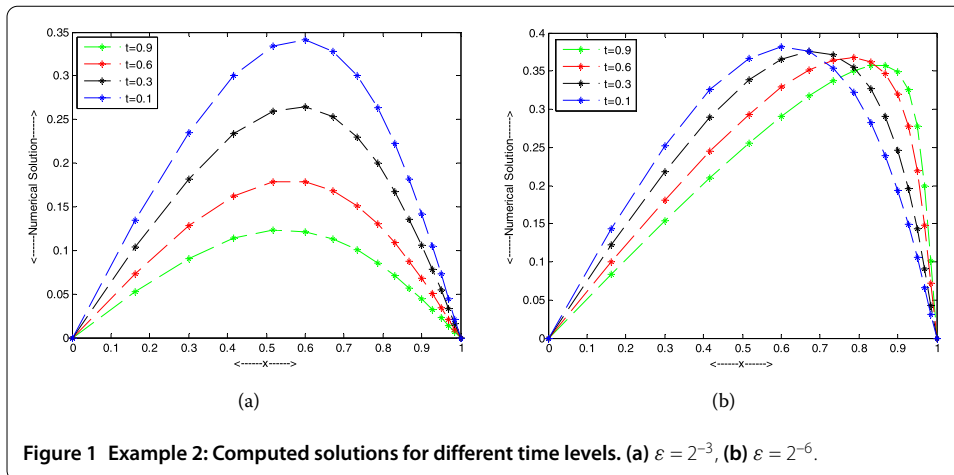


Figure 1 Example 2: Computed solutions for different time levels. (a) $\varepsilon = 2^{-3}$, (b) $\varepsilon = 2^{-6}$.

$$u(-1, t) = u(1, t) = 0, \quad t > 0. \tag{6.10b}$$

The computed numerical solutions for this example are presented in Figure 2(a)-(f) for different value of the parameters. In our first computation, we compute the results for a fixed value of β and different value of ε at different time levels. We take $\beta = 1$, $t = 0.0, 0.5, 1.0, 1.5$ and $\varepsilon = 0.005, 0.05, 0.5$, respectively. The corresponding graphical solutions are presented in Figure 2(a)-(c). In our second computation, we compute the results for a fixed value of ε and different valued of β at different time levels. We choose $\varepsilon = 0.2$, $t = 0.0, 0.5, 1.0, 1.5$ and $\beta = 1.5, 2.5, 5.0$, respectively. The corresponding graphical results are presented in Figure 2(d)-(f). The numerical solutions, as presented in Figure 2(a)-(f), are consistent with those illustrated in [8, 20]. In Figure 2(a)-(c), the results exhibit that the numerical diffusion is dominated with the increasing diffusion coefficient ε , whereas the reaction is gradually dominant with the increasing coefficient β as shown in Figure 2(d)-(f). Thus, the computed and numerical solutions are in good agreement with the solution in the literature and the physical behavior of the differential equation.

Example 4 The one-dimensional GBHE is given by the following form:

$$\varepsilon u_{xx} = u_t + \alpha u^\delta u_x + \beta u(u^\delta - 1)(u^\delta - \gamma), \quad a < x < b, t > 0, \tag{6.11}$$

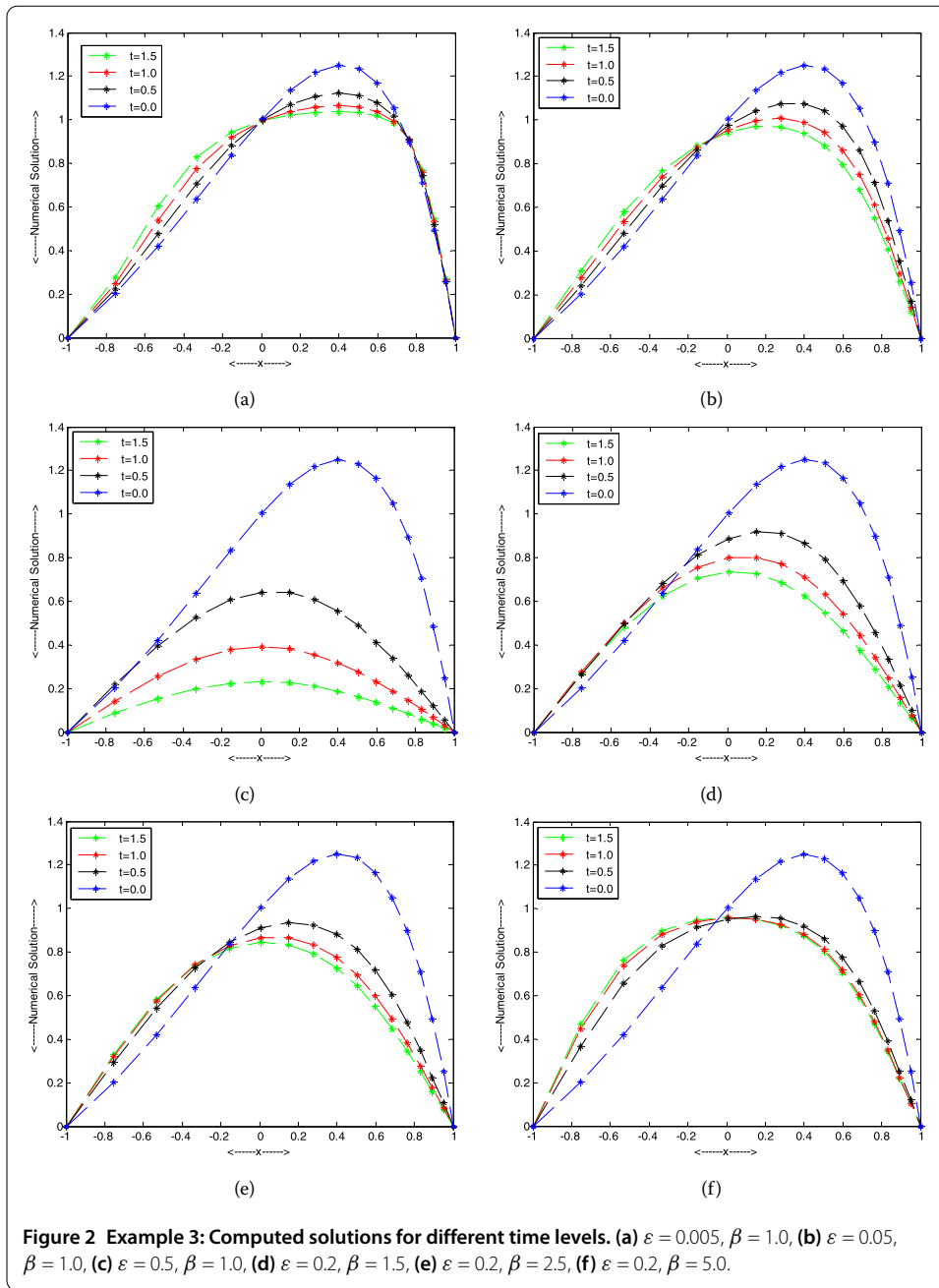
where $u = u(x, t)$ is sufficiently differentiable function, $[a, b] = [0, 1]$, $\varepsilon > 0$ is a small positive parameter, α is real parameter, $\beta \geq 0$, $\delta > 0$, $\gamma \in (0, 1)$ and $\gamma_0 = -(1 + \gamma)$. When $\alpha = 1$, $\beta = 0$, $\delta = 1$ and $0 < \varepsilon \ll 1$, (6.11) is the well-known Burgers equation [21], where ε is the coefficient of viscosity and $R_e = \varepsilon^{-1} > 0$ is the Reynolds Number.

The initial condition associated with differential equation (6.11) is given by

$$u(x, 0) = \left[\frac{\gamma}{2} + \frac{\gamma}{2} \tanh(a_1 x) \right]^{1/\delta}, \quad a \leq x \leq b, \tag{6.12}$$

and the boundary condition associated with the (6.11) are given by

$$u(a, t) = \left[\frac{\gamma}{2} + \frac{\gamma}{2} \tanh(a_1(a - a_2 t)) \right]^{1/\delta}, \quad t \geq 0, \tag{6.13}$$



$$u(b, t) = \left[\frac{\gamma}{2} + \frac{\gamma}{2} \tanh(a_1(b - a_2t)) \right]^{1/\delta}, \quad t \geq 0, \tag{6.14}$$

the exact solution [7] of (6.11) is given by

$$u(x, t) = \left[\frac{\gamma}{2} + \frac{\gamma}{2} \tanh(a_1(x - a_2t)) \right]^{1/\delta}, \quad t \geq 0, \tag{6.15}$$

where

$$\varepsilon = 1, \quad a_1 = \frac{-\alpha\delta + \delta\sqrt{\alpha^2 + 4\beta(1 + \delta)}}{4(1 + \delta)}\gamma,$$

Table 10 Example 4: Case 4.1: Maximum absolute errors

x	t	$\delta = 1$	$\delta = 2$	$\delta = 4$
0.1	0.1	6.7654(-17)	6.3838(-16)	6.4393(-15)
	0.5	4.6404(-17)	4.8919(-16)	4.6352(-15)
	0.9	4.7054(-17)	4.5797(-17)	4.9682(-15)
0.5	0.1	2.9816(-17)	3.4001(-16)	3.2752(-15)
	0.5	4.2284(-17)	4.3716(-16)	4.2466(-15)
	0.9	4.2609(-17)	4.2674(-16)	4.3854(-15)
0.9	0.1	1.0842(-19)	6.9389(-18)	2.7756(-17)
	0.5	5.4210(-19)	6.9389(-18)	5.5511(-17)
	0.9	5.4210(-19)	6.9389(-18)	5.5511(-17)

Table 11 Example 4: Case 4.2: Maximum absolute errors

x	t	$\beta = 10$	$\beta = 100$	$\beta = 200$
0.1	0.1	6.4393(-15)	6.6946(-14)	6.7590(-13)
	0.5	2.6867(-14)	4.4409(-14)	2.6479(-14)
	0.9	8.3267(-16)	8.8818(-15)	8.4044(-14)
0.5	0.1	5.2736(-15)	4.6241(-14)	4.5314(-13)
	0.5	9.9809(-14)	7.0166(-14)	6.7590(-13)
	0.9	7.0499(-15)	6.9666(-14)	7.0732(-13)
0.9	0.1	1.1102(-16)	7.7716(-16)	7.6050(-15)
	0.5	2.6423(-14)	1.3878(-15)	1.4044(-14)
	0.9	1.6653(-16)	1.3878(-15)	1.4044(-14)

$$a_2 = \frac{\alpha\gamma}{(1 + \delta)} + \frac{(1 + \delta - \gamma)(\alpha + \sqrt{\alpha^2 + 4\beta(1 + \delta)})}{2(1 + \delta)}.$$

The following cases have been discussed for different values of the parameters α, β, γ and δ which are involved in Eq. (6.11).

Case 4.1: In this case, we consider $\alpha = 1, \beta = 1, \gamma = 0.001$ and mesh ratio $\sigma = 0.85$. We have computed the numerical results for different time levels, namely $t = 0.1, 0.5, 1.0$ with step size $k = 0.0001$ and $\delta = 1, 2, 4$, respectively. Maximum absolute errors have been presented for $x = 0.1, 0.5, 0.9$ in Table 10.

Case 4.2: In this case, we consider $\alpha = 1, \delta = 8, \gamma = 10^{-4}$ and mesh ratio $\sigma = 0.9$. We have computed the numerical results for fixed time level $t = 1.0$ with step size $k = 0.0001$ and $\beta = 10, 100, 200$. Maximum absolute errors have been presented for $x = 0.1, 0.2, 0.3, 0.4, 0.5$ in Table 11.

Case 4.3: In this case, we consider $\alpha = 5, \beta = 10, \delta = 4$. and mesh ratio $\sigma = 0.9$. We have computed the numerical results for fixed time level $t = 0.5$ with step size $k = 0.0001$ and $\gamma = 10^{-2}, 10^{-3}, 10^{-4}$. Maximum absolute errors have been presented for $x = 0.1, 0.2, 0.3, 0.4, 0.5$ in Table 12.

Case 4.4: In this case, we consider $\alpha = 1, \beta = 0$ and mesh ratio $\sigma = 0.9$. We consider the initial and boundary conditions are given by

$$u(x, 0) = \frac{2\varepsilon \sin(\pi x)}{2 + \cos(\pi x)}, \quad 0 \leq x \leq 1, \tag{6.16}$$

$$u(0, t) = u(1, t) = 0, \quad t \geq 0. \tag{6.17}$$

The exact solution [9] is given by

$$u(x, t) = \frac{2\varepsilon\pi \exp(-\varepsilon\pi^2 t \sin(\pi x))}{2 + \exp(-\varepsilon\pi^2 t \cos(\pi x))}. \tag{6.18}$$

Table 12 Example 4: Case 4.3: Maximum absolute errors

x	t	$\gamma = 10^{-2}$	$\gamma = 10^{-3}$	$\gamma = 10^{-4}$
0.1	0.1	1.1852(-13)	6.4193(-14)	7.1360(-15)
	0.5	1.1358(-13)	3.6082(-14)	1.0680(-15)
	0.9	1.0858(-13)	7.6883(-15)	8.4099(-15)
0.5	0.1	8.8096(-14)	5.2708(-14)	6.9000(-14)
	0.5	8.4543(-14)	7.0194(-14)	6.9375(-14)
	0.9	8.1157(-14)	6.8168(-14)	4.8003(-14)
0.9	0.1	2.3870(-15)	8.8818(-16)	1.4017(-15)
	0.5	2.2760(-15)	1.3878(-15)	1.4017(-15)
	0.9	2.2204(-15)	1.4155(-15)	7.7716(-16)

Table 13 Example 4: Case 4.4: Maximum absolute errors $\alpha = 1, \beta = 0$

$N + 1$	Proposed method (3.6)			Method given in [4]		
	$R_e = 10^2$	$R_e = 10^4$	$R_e = 10^6$	$R_e = 10^2$	$R_e = 10^4$	$R_e = 10^6$
8	8.8258(-06)	1.9258(-09)	1.0430(-13)	4.1061(-04)	8.3710(-08)	8.4373(-12)
16	4.9239(-07)	9.7076(-11)	1.0463(-14)	1.1067(-04)	2.2489(-08)	2.2700(-12)
32	4.2004(-08)	7.3269(-12)	9.9642(-16)	2.7680(-05)	5.7437(-09)	5.7920(-13)
64	1.0396(-08)	1.2489(-12)	1.3421(-16)	6.9473(-06)	1.4564(-09)	1.4698(-13)

Results are computed for fixed time level $t = 1.0$ and for $\delta = 1$. Maximum absolute errors have been presented for $R_e = \varepsilon^{-1} = 10^2, 10^4, 10^6$ in Table 13.

Example 5 We consider equation (6.11) with initial and boundary conditions are given in Mittal and Jiwari [18], namely

$$u(x, 0) = \sin(\pi x), \quad 0 < x < 1, \tag{6.19a}$$

$$u(0, t) = u(1, t) = 0, \quad t > 0. \tag{6.19b}$$

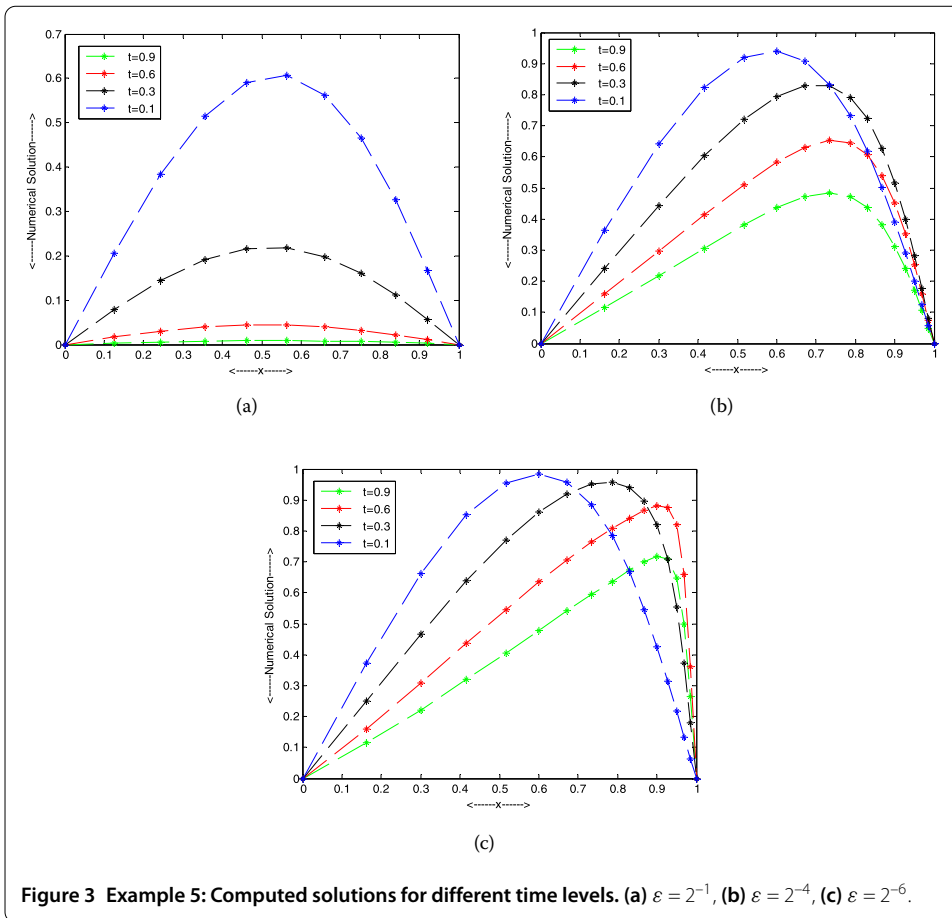
In our computation, we find solutions at different time levels for various decreasing values of ε . We take $t = 0.1, 0.3, 0.6, 0.9$ with step size $k = 0.001$ and $\varepsilon = 2^{-1}, 2^{-4}, 2^{-6}$, respectively. The computed solutions are interpreted graphically in Figure 3(a)-(c) for $\alpha = 1, \beta = 1, \delta = 1$ and $\gamma = 0.5$. We notice that, for a fixed value of ε as time t increases, the solutions curves fall to zero. Thus, the obtained solutions explain the nature of equation (6.11) faithfully in terms of diffusivity versus time. The approximate numerical solutions obtained by the present method exhibit correct physical behavior for several values of ε and t . Similar patterns have been depicted in [8].

Example 6 We consider equation (6.11) with initial and boundary conditions as given in Kaushik [19], namely

$$u(x, 0) = 1 - \cos(x), \quad 0 < x < 1, \tag{6.20a}$$

$$u(0, t) = u(1, t) = 0, \quad t > 0. \tag{6.20b}$$

We computed numerical solutions for different time levels for various decreasing values of ε . We take $t = 0.2, 0.4, 0.6, 0.8$ with step size $k = 0.001$ and $\varepsilon = 2^{-4}, 2^{-6}, 2^{-7}$, respectively. The obtained solutions have been plotted in Figure 4(a)-(c) for $\alpha = 3, \beta = 9.8, \delta = 1$ and $\gamma = 0.7$. The graphs obtained in Figure 4(a)-(c) capture the nature of equation (6.11) faithfully



in terms of diffusivity versus time. As the time increases, solution curves decreases to zero. For the decreasing value of ϵ , curves become steeper and propagate to the right which is the behavior of shocks waves. Similar patterns have been presented in [8, 19] also.

Example 7 The coupled viscous nonlinear Burgers equation is given by the following form:

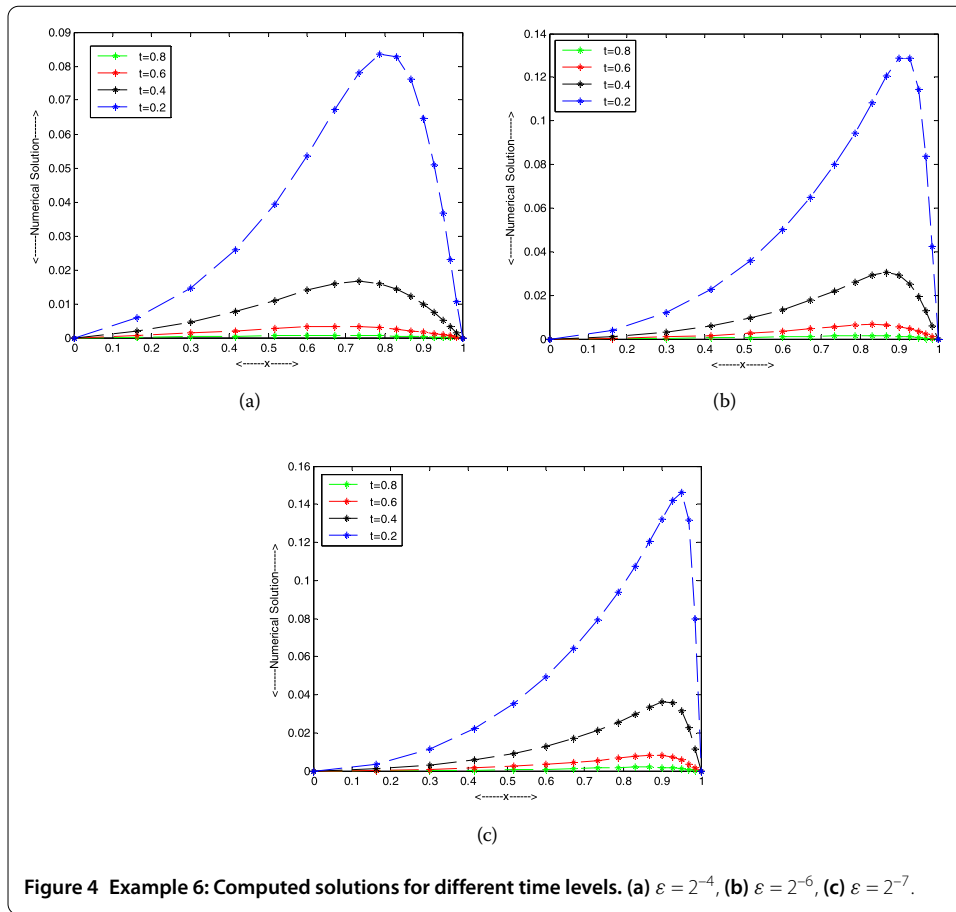
$$\epsilon \frac{\partial^2 u}{\partial x^2} = \frac{\partial u}{\partial t} + \alpha_1 u \frac{\partial u}{\partial x} + \alpha_2 \frac{\partial(uv)}{\partial x}, \quad a < x < b, t > 0, \tag{6.21}$$

$$\epsilon \frac{\partial^2 v}{\partial x^2} = \frac{\partial v}{\partial t} + \beta_1 v \frac{\partial v}{\partial x} + \beta_2 \frac{\partial(uv)}{\partial x}, \quad a < x < b, t > 0. \tag{6.22}$$

Here $0 < \epsilon \ll 1$ is the viscosity, $R_e = \epsilon^{-1} > 0$ is the Reynolds number, α_1 and β_1 are real constants, α_2 and β_2 are arbitrary constants depending on the system parameters [12]. The coupled Burgers equations (6.21) and (6.22) represent a system of one-space dimensional quasi-linear parabolic equations with two unknown variables u and v .

The initial condition associated with differential equations (6.21) and (6.22) is given by

$$u(x, 0) = v(x, 0) = \sin x, \quad -\pi \leq x \leq \pi, \tag{6.23}$$



and the boundary conditions associated with (6.21), (6.22) are given by

$$u(-\pi, t) = u(\pi, t) = 0, \quad 0 \leq t \leq T, \tag{6.24}$$

$$v(-\pi, t) = v(\pi, t) = 0, \quad 0 \leq t \leq T. \tag{6.25}$$

The values of parameters are given by $\alpha_1 = \beta_1 = -2$ and $\alpha_2 = \beta_2 = 1$. The exact solutions of equations (6.21), (6.22) are $u(x, t) = e^{-t} \sin x$ and $v(x, t) = e^{-t} \sin x$ (see [22]).

In this example, we choose a uniform mesh ($\sigma = 1$) to compute the numerical solutions for different values of the parameters $\varepsilon, \alpha_1, \alpha_2, \beta_1$ and β_2 with different values of h and k . In our first computation, we choose $\varepsilon = 1, \alpha_1 = \beta_1 = -2, \alpha_2 = \beta_2 = 1, h = \frac{2\pi}{100}, k = 0.01$ and maximum absolute errors are computed at various time levels from $t = 0.5$ to 3.0 . The corresponding results are tabulated in Table 14. In our second computation, the maximum absolute errors are computed at $t = 1.0$ and $t = 2.0$ for a fixed $\lambda = \frac{1.6}{4\pi^2}, \varepsilon = 1, \alpha_1 = \beta_1 = -2, \alpha_2 = \beta_2 = 1$. Numerical results are presented in Table 15.

Example 8 We consider the coupled Burgers equations (6.21), (6.22) with the following initial and boundary conditions:

$$u(x, 0) = v(x, 0) = \cos(\pi x), \quad 0 \leq x \leq 1 \tag{6.26}$$

Table 14 Example 7: Maximum absolute error at $\varepsilon = 1, \alpha_1 = \beta_1 = -2, \alpha_2 = \beta_2 = 1, h = 2\pi/100, k = 0.01$

t	Proposed method (4.28)		Method discussed in [11]	
	u	v	u	v
0.5	2.5045(-06)	2.5045(-06)	1.5168(-04)	1.5168(-04)
1.0	3.0373(-06)	3.0373(-06)	1.8397(-04)	1.8397(-04)
2.0	2.2330(-06)	2.2330(-06)	1.3525(-04)	1.3525(-04)
3.0	1.2296(-06)	1.2296(-06)	7.4601(-05)	7.4601(-05)

Table 15 Example 7: Maximum absolute errors, $\varepsilon = 1, \alpha_1 = \beta_1 = -2, \alpha_2 = \beta_2 = 1, \lambda = 1.6/4\pi^2$

$N + 1$		Proposed method (4.28)		Method given in [10]	
		$t = 1.0$	$t = 2.0$	$t = 1.0$	$t = 2.0$
8	u	5.7826(-04)	4.2579(-05)	7.4756(-04)	6.1386(-04)
	v	5.7826(-04)	4.2579(-05)	7.4756(-04)	6.1386(-04)
16	u	3.5478(-05)	2.6105(-07)	5.1124(-05)	3.8618(-05)
	v	3.5478(-05)	2.6105(-07)	5.1124(-05)	3.8618(-05)
32	u	2.2070(-06)	1.6238(-06)	3.3516(-06)	2.4173(-06)
	v	2.2070(-06)	1.6238(-06)	3.3516(-06)	2.4173(-06)
64	u	1.3777(-07)	1.0137(-07)	2.2035(-07)	1.5114(-07)
	v	1.3777(-07)	1.0137(-07)	2.2035(-07)	1.5114(-07)
128	u	8.6048(-09)	6.3339(-09)	1.3837(-08)	9.3878(-09)
	v	8.6048(-09)	6.3339(-09)	1.3837(-08)	9.3878(-09)

Table 16 Example 8: Maximum absolute errors at $t = 1, \alpha_1 = \beta_1 = 2, \alpha_2 = \beta_2 = -1, \lambda = 3.2$

$N + 1$		Proposed method (4.28)			Method given in [10]		
		$R_e = 100$	$R_e = 200$	$R_e = 250$	$R_e = 100$	$R_e = 200$	$R_e = 250$
8	u	6.3075(-06)	3.9152(-06)	3.2823(-06)	8.0563(-06)	4.3982(-06)	3.5838(-06)
	v	6.3075(-06)	3.9152(-06)	3.2837(-06)	8.0563(-06)	4.3982(-06)	3.5838(-06)
16	u	4.1145(-07)	2.4266(-07)	2.0268(-07)	5.0129(-07)	2.8249(-07)	2.2612(-07)
	v	4.1145(-05)	2.4266(-07)	2.0268(-07)	5.0129(-07)	2.8249(-07)	2.2612(-07)
32	u	2.5696(-08)	1.5236(-08)	1.2647(-08)	3.1617(-08)	1.7629(-08)	1.4379(-08)
	v	2.5696(-08)	1.5236(-08)	1.2647(-08)	3.1617(-08)	1.7629(-08)	1.4379(-08)
64	u	1.6133(-09)	9.5490(-10)	7.9187(-10)	1.9755(-09)	1.1015(-09)	8.9877(-10)
	v	1.6133(-09)	9.5490(-10)	7.9187(-10)	1.9755(-09)	1.1015(-09)	8.9877(-10)
128	u	1.0082(-10)	5.9683(-11)	4.9531(-11)	1.2337(-10)	6.8803(-11)	5.6159(-11)
	v	1.0082(-10)	5.9683(-11)	4.9531(-11)	1.2337(-10)	6.8803(-11)	5.6159(-11)

and

$$u(0, t) = v(0, t) = e^{-\varepsilon\pi^2 t}, \quad 0 \leq t \leq T, \tag{6.27}$$

$$u(1, t) = v(1, t) = -e^{-\varepsilon\pi^2 t}, \quad 0 \leq t \leq T. \tag{6.28}$$

In this example, we choose a uniform mesh size to compute the numerical solution for different parameters $\alpha_1 = \beta_1 = 2$ and $\alpha_2 = \beta_2 = -1$, the exact solutions of equations (6.21), (6.22) are $u(x, t) = e^{-\varepsilon\pi^2 t} \cos(\pi x)$ and $v(x, t) = e^{-\varepsilon\pi^2 t} \cos(\pi x)$.

We computed the maximum absolute errors at time $t = 1$ for a fixed $\lambda = 3.2$ and the parameters $\alpha_1 = \beta_1 = 2, \alpha_2 = \beta_2 = -1$ with the decreasing values of h and k , and different values of $R_e = \varepsilon^{-1}$. The numerical results are reported in Table 16. The graphs of numerical and exact solutions at $t = 1$ are plotted in Figure 5(a)-(c).

Example 9 Equation (5.1) is solved, for which an exact solution is $u(r, t) = e^{-t} \sinh r$. In this example, we choose uniform mesh to compute the maximum absolute errors at time

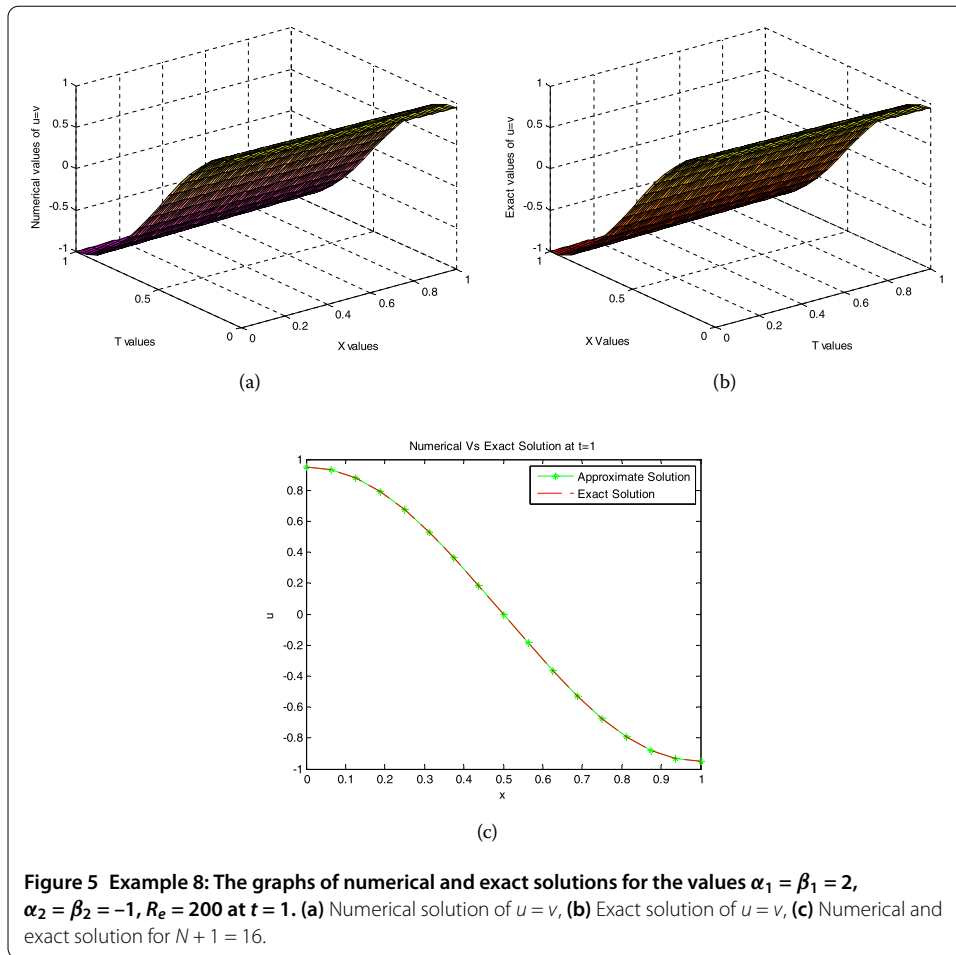


Figure 5 Example 8: The graphs of numerical and exact solutions for the values $\alpha_1 = \beta_1 = 2$, $\alpha_2 = \beta_2 = -1$, $R_e = 200$ at $t = 1$. (a) Numerical solution of $u = v$, (b) Exact solution of $u = v$, (c) Numerical and exact solution for $N + 1 = 16$.

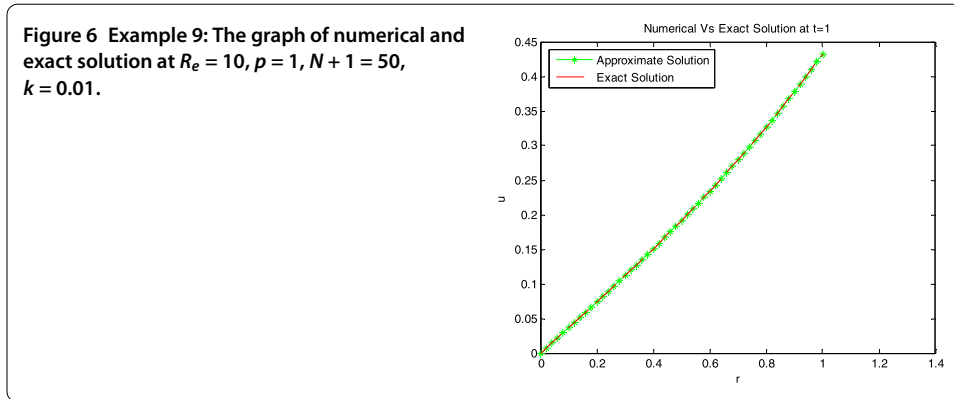
Table 17 Example 9: Maximum absolute errors at $t = 1$, $k = 0.01$

$N + 1$	$p = 1$		$p = 2$	
	$R_e = 10$	$R_e = 100$	$R_e = 10$	$R_e = 100$
50	1.6813(-06)	4.6778(-06)	1.5631(-06)	4.6698(-06)
60	1.4553(-06)	4.6745(-06)	1.3410(-06)	4.6676(-06)
70	1.2087(-06)	4.6677(-06)	1.1388(-06)	4.6634(-06)
80	9.1317(-07)	4.6789(-06)	8.5845(-07)	4.6621(-06)
90	6.1444(-07)	4.6794(-06)	5.4123(-07)	4.6623(-06)

$t = 1$ for a fixed $k = 0.01$, $p = 1$ and 2 and for various values of $R_e = \varepsilon^{-1}$. The corresponding numerical results are reported in Table 17. The graphs of numerical and exact solutions at $t = 1$ are plotted in Figure 6.

7 Final remarks

In this article, we have presented a new two-level implicit method based on spline in compression approximations of accuracy $O(kh_l + h_l^3)$ for the numerical solution of quasi-linear parabolic partial differential equation in one spatial dimension. Mathematical formulation of the proposed scheme using three spatial grid points is discussed in detail. We have extended the proposed scheme to the system of quasi-linear parabolic equations. The stability analysis of the present numerical approach for one-dimensional linear



convection-diffusion equation and fourth-order parabolic equation is presented. We have solved several benchmark problems using proposed method and it successfully provides highly accurate solutions in different settings of parameters. For different values of the parameters involved in GBFE, we have computed maximum absolute errors in Example 1 and we observe that our method is giving more accurate results than the results obtained by [5, 23–25]. In Examples 2 and 3, we have plotted the graphs (Figure 1(a)-(b) and Figure 2(a)-(f)) at different time levels and for different values of parameters in GBFE, which exhibits that the numerical diffusion is dominated with the increasing diffusion coefficient ε , whereas the reaction is gradually dominant with the increasing coefficient β . Similar patterns of graphs have been presented in [8, 18–20]. We have compared the computed numerical solutions with the exact solutions of GBHE in Example 4. Maximum absolute errors have been tabulated. The results obtained are quite good and competent with exact solution available in the literature. In Examples 5 and 6, we have plotted the graphs (Figure 3(a)-(c) and Figure 4(a)-(c)) at different time levels and different values of parameters involved in GBHE which describes that solution curves decreases to zero as time increases and for small value of ε , solution curves behave like a shocks waves. We have computed maximum absolute errors for coupled viscous nonlinear Burgers’ equation in Examples 7 and 8. On comparing the nature of computed solution with the computed solutions available in [10, 11], we obtained better results by our scheme. Also we have plotted graphs (Figure 5(a)-(c)) of exact versus numerical solution $t = 1$. In Example 9, we have solved singular parabolic partial differential equation in polar coordinates and obtained maximum absolute errors for cylindrical and spherical case. At $t = 1$, we have plotted graph (Figure 6) of numerical versus exact solution for Example 9. It can be observed that the approximate solution computed with our scheme and exact solutions are identical.

Acknowledgements

The authors thank the reviewers for their valuable comments and suggestions, which substantially improved the standard of the paper. This research work is supported by CSIR-SRF, Grant No: 09/045(1161)/2012-EMR-I.

Competing interests

The authors declare that they have no competing interest.

Authors’ contributions

All authors drafted the manuscript, and they read and approved the final version.

Author details

¹Department of Applied Mathematics, South Asian University, Akbar Bhawan, Chanakyapuri, New Delhi 110021, India.

²Department of Mathematics, Faculty of Mathematical Sciences, University of Delhi, Delhi, 110007, India.

Publisher's Note

Springer Nature remains neutral with regard to jurisdictional claims in published maps and institutional affiliations.

Received: 9 May 2017 Accepted: 10 July 2017 Published online: 01 August 2017

References

1. Fisher, RA: The wave of advance of advantageous genes. *Annu. Eugen.* **7**, 353-369 (1937)
2. Kolmogorov, AN, Petrovskii, IG, Piskunov, NS: A study of the equation of diffusion with increase in the quantity of matter, and its application to a biological problem. *Bjul. Moskovskogo Gos. Univ.* **1**(7), 1-26 (1937)
3. Satsuma, J, Ablowitz, M, Fuchssteiner, B, Kruskal, M: *Topics in Soliton Theory and Exactly Solvable Nonlinear Equations*. World Scientific, Singapore (1987)
4. Bratsos, AG: A fourth order improved numerical scheme for the generalized Burgers-Huxley equation. *Am. J. Comput. Math.* **1**, 152-158 (2011)
5. Mohammadi, R: Spline solution of the generalized Burgers'-Fisher equation. *Appl. Anal.* **91**(12), 2189-2215 (2011)
6. Zhang, R, Yu, X, Zhao, G: The local discontinuous Galerkin method for Burgers-Huxley and Burgers-Fisher equations. *Appl. Math. Comput.* **218**, 8773-8778 (2012)
7. Macias-Diaz, JE: On an exact numerical simulation of solitary wave-solutions of the Burgers-Huxley equation through Cardano's method. *BIT Numer. Math.* **54**, 763-776 (2014)
8. Mittal, RC, Tripathi, A: Numerical solutions of generalized Burgers-Fisher and generalized Burgers-Huxley equations using collocation of cubic B-splines. *Int. J. Comput. Math.* **92**(5), 1053-1077 (2015)
9. Mohanty, RK, Dai, W, Liu, D: Operator compact method of accuracy two in time and four in space for the solution of time independent Burgers-Huxley equation. *Numer. Algorithms* **70**, 591-605 (2015)
10. Jain, MK, Jain, RK, Mohanty, RK: High order difference methods for system of 1-D non-linear parabolic partial differential equations. *Int. J. Comput. Math.* **37**, 105-112 (1990)
11. Mittal, RC, Jiwari, R: Differential quadrature method for numerical solution of coupled viscous Burgers' equations. *Int. J. Comput. Methods Eng. Sci. Mech.* **13**, 88-92 (2012)
12. Mohanty, RK, Dai, W, Han, F: Compact operator method of accuracy two in time and four in space for the numerical solution of coupled viscous Burgers' equations. *Appl. Math. Comput.* **256**, 381-393 (2015)
13. Talwar, J, Mohanty, RK, Singh, S: A new spline in compression approximation for one space dimensional quasilinear parabolic equations on a variable mesh. *Appl. Math. Comput.* **260**, 82-96 (2015)
14. Mohanty, RK: An implicit high accuracy variable mesh scheme for 1D non-linear singular parabolic partial differential equations. *Appl. Math. Comput.* **186**, 219-229 (2007)
15. Mohanty, RK, Setia, N: A new high order compact off-step discretization for the system of 3D quasi-linear elliptic partial differential equations. *Appl. Math. Model.* **37**, 6870-6883 (2013)
16. Mohanty, RK, Jain, MK: High-accuracy cubic spline alternating group explicit methods for 1D quasi-linear parabolic equations. *Int. J. Comput. Math.* **86**, 1556-1571 (2009)
17. Mohanty, RK: A variable mesh C-SPLAGE method of accuracy $O(k^2h^{-1} + kh + h^3)$ for 1D nonlinear parabolic equations. *Appl. Math. Comput.* **213**, 79-91 (2009)
18. Mittal, RC, Jiwari, R: Numerical study of Burgers-Huxley equation by differential quadrature method. *Int. J. Appl. Math. Mech.* **5**, 1-9 (2009)
19. Kaushik, A: Pointwise uniformly convergent numerical treatment for the non-stationary Burgers-Huxley using grid equidistribution. *Int. J. Comput. Math.* **84**(10), 1527-1546 (2007)
20. Zhao, T, Li, C, Zang, Z, Wu, Y: Chebyshev-Legendre pseudo-spectral method for generalized Burgers-Fisher equation. *Appl. Math. Model.* **36**(3), 1046-1056 (2012)
21. Burgers, JM: A mathematical model illustrating the theory of turbulence. *Adv. Appl. Mech.* **1**, 171-199 (1948)
22. Kaya, D: An explicit solution of coupled viscous Burgers' equations by the decomposition method. *Int. J. Math. Math. Sci.* **27**, 675-680 (2001)
23. Sari, M, Gürarslan, G, Zeytinoglu, A: High-order finite difference schemes for the solution of the generalized Burgers'-Fisher equation. *Commun. Numer. Methods Eng.* **27**(8), 1296-1308 (2011)
24. Zhu, C-G, Kang, W-S: Numerical solution of Burgers'-Fisher equation by cubic B-spline quasi-interpolation. *Appl. Math. Comput.* **216**, 2679-2686 (2010)
25. Sari, M, Gürarslan, G, Dag, I: A compact finite difference method for the solution of the generalized Burgers'-Fisher equation. *Numer. Methods Partial Differ. Equ.* **26**, 125-134 (2010)

Submit your manuscript to a SpringerOpen[®] journal and benefit from:

- Convenient online submission
- Rigorous peer review
- Open access: articles freely available online
- High visibility within the field
- Retaining the copyright to your article

Submit your next manuscript at ► springeropen.com
